Specific triazine herbicides induce amyloid β 42 production

Erik **PORTELIUS**[a], Emilie **DURIEU**[b], Marion **BODIN**[b], Morgane **CAM**[b], Josef **PANNEE**[a], Charlotte **LEUXE**[c], Aloïse **MABONDZO**[c], Nassima **OUMATA**[b], Hervé **GALONS**[b,d], Jung Yeol **LEE**[e], Young-Tae **CHANG**[e], Kathrin **STÜBER**[f], Philipp **KOCH**[f], Gaëlle **FONTAINE**[g], Marie-Claude **POTIER**[g], Antigoni **MANOUSOPOULOU**[h], Spiros **GARBIS**[h], Adrian **COVACI**[i], Debby **VAN DAM**[j,k], Peter **DE DEYN**[j,k], Frank **KARG**[l], Marc **FLAJOLET**[m], Chiori **OMORI**[n], Saori **HATA**[n], Toshiharu **SUZUKI**[n], Kaj **BLENNOW**[a], Henrik **ZETTERBERG**[a,o] and Laurent **MEIJER**[b, l]

[a]Clinical Neurochemical Laboratory, Institute of Neuroscience & Physiology, University of Gothenburg, 41345 Göteborg, Sweden; [b]ManRos Therapeutics, Centre de Perharidy, 29680 Roscoff, France; [c]CEA, Direction des Sciences du Vivant, Service de Pharmacologie & d'Immunoanalyse, 91191 Gif-sur-Yvette, France; [d]Laboratoire de Pharmacochimie, INSERM U1022, Université Paris-Descartes, 75006 Paris, France; [e]Department of Chemistry, National University of Singapore, Laboratory of Bioimaging Probe Development, Biopolis, Singapore 138667; [f]Institute of Reconstructive Neurobiology, University of Bonn, 53127 Bonn, Germany; [g]Sorbonne Universités, UPMC Université Paris 06 UMR S1127, Inserm U1127, CNRS UMR7225, ICM, 75013 Paris, France; [h]Faculty of Medicine, Cancer Sciences & Clinical and Experimental Medicine, University of Southampton, Southampton, SO17 1BJ, UK; [i]Toxicological Center, University of Antwerp, 2610 Wilrijk, Belgium; [j]Laboratory of Neurochemistry & Behaviour, Department of Biomedical Sciences, Institute Born-Bunge, 2610 Wilrijk, Belgium; [k]University of Groningen, University Medical Center Groningen, Department of Neurology & Alzheimer Research Center, Groningen, 9713GZ, The Netherlands; [l]HPC Envirotec S.A./France, Noyal-Châtillon sur Seiche, 35230 Saint-Erblon, France; [m]Laboratory of Molecular & Cellular Neuroscience, The Rockefeller University, New York, NY 10021, USA; [n]Laboratory of Neuroscience, Graduate School of Pharmaceutical Sciences, Hokkaido University, Sapporo 060-0812, Japan; UCL Institute of Neurology, London, WC1N 3BG, UK.

Running title: Triazine herbicides induce Aβ42 production

1 Corresponding author: Laurent Meijer, ManRos Therapeutics, 29680 Roscoff, France. Tel. +33.6.08.60.58.34, <meijer@manros-therapeutics.com>

Key words

Alzheimer's disease, amyloid precursor protein, amyloid β, $A\beta_{42}/A\beta_{40}$ ratio, herbicides, triazines, human chemical exposome, alzheimerogen.

ABSTRACT

Proteolytic cleavage of the amyloid precursor protein (AβPP) by secretases leads to extracellular release of amyloid β (Aβ) peptides. Increased production of $A\beta_{42}$ over $A\beta_{40}$ and aggregation into oligomers and plaques constitute an Alzheimer's disease (AD) hallmark. Identifying products of the 'human chemical exposome' (HCE) able to induce $A\beta_{42}$ production may be a key to understand some of the initiating causes of AD and to generate non-genetic, chemically-induced AD animal models. A cell model was used to screen HCE libraries for $A\beta_{42}$ inducers. Out of 3500+ compounds, six triazine herbicides were found that induced a β- and γ-secretases -dependent, 2-10 fold increase in the production of extracellular $A\beta_{42}$ in various cell lines, primary neuronal cells and neurons differentiated from human induced pluripotent stem cells (iPSCs). Immunoprecipitation/mass spectrometry analyses show enhanced production of Aβ peptides cleaved at positions 42/43, and reduced production of peptides cleaved at positions 38 and lower, a characteristic of AD. Neurons derived from iPSCs obtained from a familial AD (FAD) patient (AβPP K724N) produced more $A\beta_{42}$ vs. $A\beta_{40}$ than neurons derived from healthy controls iPSCs (AβPP WT). Triazines enhanced $A\beta_{42}$ production in both control and AD neurons. Triazines also shifted the cleavage pattern of alcadeinα, another γ-secretase substrate, suggesting a direct effect of triazines on γ-secretase activity. In conclusion, several widely used triazines enhance the production of toxic, aggregation prone $A\beta_{42}/A\beta_{43}$ amyloids, suggesting the possible existence of environmental "Alzheimerogens" which may contribute to the initiation and propagation of the amyloidogenic process in late-onset AD.

INTRODUCTION

Proteolytic processing of AβPP by β- and γ-secretases leads to the production of various Aβ peptides, including the 42-amino acid form ($A\beta_{42}$) which plays a crucial role in AD [1-3]. The action of β-secretase first leads to a soluble fragment (sAβPP) and a membrane-bound fragment (βCTF, β-carboxyl-terminal fragment). γ-Secretase then cleaves

the βCTF, leading to the generation of Aβ peptides of various lengths. Aβ peptides tend to aggregate as extracellular oligomers and ultimately as plaques, one of the clinical hallmarks of AD.

$A\beta_{40}$ is the most abundantly produced Aβ peptide. Considerable data indicates that generation of the aggregation-prone $A\beta_{42}$ strongly correlates with the onset and development of AD. In early-onset AD (EOAD) (<1% of all cases), mutations in AβPP, or the γ-secretase subunits PSEN1 & PSEN2 [review in 4], all lead to enhanced $A\beta_{42}$ production and/or increased $A\beta_{42}/A\beta_{40}$ ratio, a critical factor in AD pathology initiation [5]. Increased $A\beta_{42}/A\beta_{40}$ ratio is also found in brain tissue in late-onset AD (LOAD) (>99% of AD cases). $A\beta_{42}$ is more toxic than $A\beta_{40}$, a consequence of its higher stability and strong tendency to oligomerize and to aggregate in plaques [6-8]. $A\beta_{43}$ is also enriched in the brain of AD patients and has been reported as a toxic, aggregation-prone amyloid, inducing strong AD phenotypes in mice [9-12].

We recently reported that some tri-substituted purines, the aftins (**A**myloid β **F**orty-**T**wo **In**ducers), trigger a robust, secretases-dependent increase in extracellular $A\beta_{42}$ production in cultured cells [13-14]. Under these conditions $A\beta_{38}$ levels dropped while $A\beta_{40}$ remained relatively stable. These results suggest that (i) such molecules might constitute new pharmacological tools to investigate the mechanisms underlying the increased $A\beta_{42}/A\beta_{40}$ ratio observed in AD, (ii) these molecules might contribute to generate a chemically induced animal model of AD [15] and (iii) some simple, low molecular weight (LMW) products in our environment might shift the $A\beta_{42}/A\beta_{40}$ ratio similarly to what is seen in AD patients and might thus contribute to the development, acceleration or even initiation of LOAD.

We therefore screened for potential $A\beta_{42}$-inducing molecules in libraries of HCE products [16-21]. We here report that a subset of the widely used triazine herbicides is able to shift Aβ production towards longer, aggregation-prone amyloid peptides ($A\beta_{42}/A\beta_{43}$) at the expense of shorter variants ($A\beta_{37}$, $A\beta_{38}$, $A\beta_{40}$). In addition, production of the shorter $A\beta_{1\text{-}16}$ and $A\beta_{1\text{-}17}$ peptides, the generation of which is dependent on β- and γ-secretase activities [22, 23], was also enhanced. This effect is observed in various cell lines, primary neuron cultures and neurons differentiated from iPSCs obtained from healthy controls or AD patients. Triazines shift the cleavage pattern of alcadeinsα, another γ-secretase substrate [24-28], in a way similar to the AβPP cleavage shift, suggesting a direct effect on γ-secretase rather than on its substrates. Altogether these data support our hypothesis that the HCE contains products able to modulate γ-secretase activity towards the production of high MW, aggregation-prone, AD-associated amyloids. Such products could be qualified as potential "Alzheimerogens"

(name by analogy with "carcinogens"). Their identification and regulation might constitute a key step in AD prevention.

MATERIAL & METHODS

Material and methods are described in full in the SI section. They include:

1. Triazines and other reagents.
2. Cell cultures: cell lines, primary neuron cultures, human iPSCs-derived neurons & HEK293-alcadeinα cells.
3. Transient transfections with AβPP truncation mutants.
4. Amyloids assays: ELISA capture assays, absolute quantification of amyloids by tandem mass spectrometry (MS/MS), amyloids profile analysis by immunoprecipitation/mass spectrometry (IP-MS).
5. Cell viability assay.

RESULTS

Screening the HCE reveals triazines as Aβ42 inducers

A library of 3500+ LMW (<1000 daltons) products representative of the HCE was assembled. All compounds were tested for their ability to trigger extracellular $A\beta_{42}$ production by N2a cells stably expressing AβPP695 (N2a-APP695), at 1, 10 and 100 μM (data not shown. A dose-dependent effect was often seen with the active compounds). In parallel, cell viability assays were run to assess cell survival at these concentrations. The vast majority of products were unable to induce $A\beta_{42}$ production. Among the few active products, we identified several triazines, a class of products which are widely used as herbicides, anti-fouling agents or flame retardants [reviews in 29]. We next tested a library of 37 triazines representing the most produced triazines worldwide (**1-37**, SI, Table S1), along with Aftin-5 (**38**) as a positive control, on both N2a-APP695 and CHO-7PA2 cells stably expressing AβPP751 (CHO-7PA2-APP751), for their ability to trigger $A\beta_{42}$ production at 1, 10 and 100 μM (SI, Table S2) (Fig. 1A).

Six triazines were found to induce more than a 3-fold change in $A\beta_{42}$ levels (Fig. 1A, 1B): ametryn, prometryn, dipropetryn, terbutryn, cybutryne, dimethametryn. As observed with aftins [13, 14], $A\beta_{42}$ production was strongly inhibited by β- (inhibitor IV) and γ-secretases (BMS 299897, DAPT) inhibitors and by a γ-secretase modulator ('Torrey Pines' compound) (the latter induces a dose-dependent increase in $A\beta_{38}$ and a decrease in $A\beta_{42}$ and $A\beta_{40}$) [30, 31] (Fig. 1C). Similarly, $A\beta_{38}$ production was strongly reduced, while $A\beta_{40}$ levels

were only modestly affected as measured by ELISA (data not shown) and by mass spectrometry (Fig. 2). Most of the triazines are metabolized in the environment and by organisms. We thus tested some of the cybutryne/terbutryn metabolites (**39-44**) (SI, Fig. S1) for their ability to trigger $A\beta_{42}$ production in N2a-APP695 and CHO-7PA2 cells. None of the tested metabolites was active as an inducer of $A\beta_{42}$ production (data not shown). We next tested a library of 236 triazines that had been synthesized as affinity chromatography reagents, for their ability to induce $A\beta_{42}$ production [32, 33]. Twenty-one of these (**45-65**) showed significant enhancement of $A\beta_{42}$ production (SI, Table S3), showing that $A\beta_{42}$ induction is an intrinsic property of some triazines. Affinity chromatography attempts with immobilized triazines did not allow us to purify specific targets, probably because of unselective hydrophobic interactions and low level expression of the specific targets (data not shown).

Results were confirmed with HEK293 stably expressing AβPPsw (data not shown) and neurons derived from human iPSCs (see below). We also analyzed the effects of triazines on primary neuronal cultures prepared from E18 OFA rat embryo brains. Neurons were exposed to 100 μM of each triazine for 18 h, and the supernatants were collected for Aβ determination by ELISA assays. The triazines also induce an increase in $A\beta_{42}$ production by primary neurons and in the $A\beta_{42}/A\beta_{40}$ ratios (Fig. 1D). $A\beta_{40}$ production remained relatively stable, while that of $A\beta_{38}$ was reduced by all triazines (Fig. 1D).

Mass spectrometric quantification and profile analysis of induced amyloids

$A\beta_{38}$, $A\beta_{40}$ and $A\beta_{42}$ were quantified in the supernatants of N2a-APP695 (Fig. 2A) and CHO-7PA2-APP751 (Fig. 2B) using LC-MS/MS [34, 35]. Like Aftins [13, 14], triazines induced a reduction in $A\beta_{38}$ levels, a slight increase or modest decrease in $A\beta_{40}$ levels and a strong increase in $A\beta_{42}$ levels (Fig. 2, bottom). $A\beta_{42}/A\beta_{40}$ ratios were strongly increased (Fig. 2, top).

We next analyzed, by IP-MS, the range of Aβ peptides produced by both cell lines exposed to each of the six triazines and aftin-5. Cell supernatants were collected and Aβ peptides were immunoprecipitated and analyzed using MALDI TOF/TOF [36]. Examples of spectra for cells exposed to terbutryn, aftin-5 and DMSO are provided in Fig. 3 and Fig. S2 (SI). Exposure to triazines increased the production of $A\beta_{1\text{-}17}$, $A\beta_{11\text{-}42}$, $A\beta_{5\text{-}42}$ and $A\beta_{1\text{-}42}$, while the production of $A\beta_{1\text{-}19}$, $A\beta_{1\text{-}27}$, $A\beta_{1\text{-}33}$, $A\beta_{1\text{-}38}$ and $A\beta_{1\text{-}39}$ was reduced (Fig. 3). Other amyloid peptides (including $A\beta_{1\text{-}40}$) showed only modest changes. $A\beta_{1\text{-}43}$, a highly neurotoxic amyloid

[9-12], was undetectable in supernatants of control cells, but strongly induced in aftin-5 and triazine-treated cells.

Neurons differentiated from human iPSCs of AD patient and healthy control

We next tested the effects of aftin-5 and the active triazines on neurons differentiated from human iPSCs derived from a healthy individual (AβPP WT, wild-type) or from a patient with familial AD (AβPP K724N mutation) [37, 38] (Fig. 4). Neurons from the healthy control were first differentiated for either 4 or 10 weeks before 24 h exposure to 100 μM aftin-5 or terbutryn (Fig. 4A). Treatment resulted in a 2-3 fold increase in $A\beta_{42}$ levels compared to neurons exposed to DMSO. $A\beta_{40}$ levels remained essentially unchanged. All six triazines were next tested on neurons derived from the control and the AD patient differentiated for 4 weeks [38, 39] (Fig. 4B). AβPP K724N neurons produced more $A\beta_{42}$ versus $A\beta_{40}$ compared to AβPP WT neurons. Addition of aftin-5 or any of the six active triazines resulted in further increase in $A\beta_{42}$ production, in both AβPP WT and AβPP K724N neurons.

AβPP sequence requirements for $A\beta_{42}$ induction by triazines

To investigate the molecular mechanisms and possible ε cleavage sites requirement for the induced $A\beta_{42}$ production, we generated six AβPP truncations (T1-T6) and expressed them transiently in N2a cells (Fig. 5A). Cells expressing these truncations were then exposed to 100 μM aftin-5 and $A\beta_{42}$ production was measured (Fig. 5B). Full-length (FL) AβPP and the first three truncations displayed enhanced $A\beta_{42}$ production (Fig. 5B). In contrast, the three remaining truncations did not allow enhanced $A\beta_{42}$ production when cells were exposed to aftin-5. Cells expressing FL AβPP and truncations T1, T3, T4 were next exposed to 100 μM of each triazine (Fig. 5C). Although T3 allowed stimulation of $A\beta_{42}$ production, T4 did not. These results reveal a strong AβPP structural requirement for enhanced $A\beta_{42}$ production induced by aftin-5 and triazines, which seems to correspond to the ε cleavage sites of AβPP by γ-secretase. At least 10 residues downstream of the $A\beta_{42}$ cleavage site are required for the full effect of aftin-5 and triazines.

Triazines and Aftin-5 shift the cleavage pattern of the γ-secretase substrates alcadeins

Like AβPP, alcadeins/calsyntenins are sequentially cleaved by secretases, first by α-secretase, leading to N- and C-terminal fragments, the latter being then cleaved by γ-secretase to an intracellular domain and the p3-Alcs peptide, in a way similar to AβPP [25, 27] (Fig. 6A) (SI, Fig. S3). We used HEK293 cells stably expressing full length alcadeinα to

investigate the effects of triazines on alcadein cleavage. Alcadeinα is first cleaved on the N-terminal side (two possible sites) followed by cleavage by γ-secretase leading to p3-Alcα35 and p3-Alcα 2N+35, the latter representing the major peptide in cultured cells (Fig. 6A). Cleavage at nearby sites (blue arrows) leads to other less abundant peptides. HEK293-alcadeinα cells were grown till 60% confluence and treated with 100 μM aftin-5 or triazines for 24 h. The secreted p3-Alcα peptides were recovered and analyzed by MALDI TOF MS (Fig. 6B).

Quantification of p3-Alcα peptides showed that, compared to the p3-Alcα peptide profile in vehicle treated cells, concentrations of the main alcadeinα peptide (p3-Alcα 2N+35) and p3-Alcα 2N+37 peptide remained stable. In contrast, both p3-Alcα 2N+34 and p3-Alcα 2N+36 concentrations dropped by ~50% and p3-Alcα 2N+38 peptide concentration increased massively (up to 28.1 fold for dimethametryn; 16.8 fold for Aftin-5) (Fig. 6C). These results show that, like for AβPP, triazines and aftin induce a shift in the cleavage pattern of Alcadeinα, another γ-secretase substrate, suggesting that these products are more likely to interact with γ-secretase rather than with its substrates.

DISCUSSION

Induction of $A\beta_{42}$ production, increase in $A\beta_{42}/A\beta_{40}$ ratio

Various drugs (fenofibrate, celecoxib, indomethacin, isoprenoids) [40], DAPT under certain conditions [41, 42], steroids [43], ceramide analogs [44], and SIN-1 (a peroxynitrite donor) [45] have been shown to increase the $A\beta_{42}/A\beta_{40}$ ratio, mostly by increasing $A\beta_{42}$ production, though never to the high level seen with aftins [13, 14]. We here show that some, but not all, widely used (though mostly banned nowadays) triazine herbicides induce a massive production of the AD-associated $A\beta_{42}$ peptide in a variety of cell types. Consequently, the $A\beta_{42}/A\beta_{40}$ ratio is increased, as observed in both familial EOAD (genetic origin) and LOAD (environmental, epigenetic origin). Detailed analysis of a variety of Aβ peptides reveals a pattern clearly associated with AD onset, such as increased $A\beta_{1\text{-}16/17}$ [22, 23], $A\beta_{1/5/11\text{-}42}$, $A\beta_{1\text{-}43}$ [9-12], and decreased $A\beta_{1\text{-}33/37/38}$ which have been shown previously to be affected in EOAD subjects [46, 47]. While the underlying molecular mechanisms for the observed chemically-induced shift of AβPP cleavage pattern remain unclear, several remarks can be made:

(1) there is a clear structure/activity relationship within triazines, as also observed with aftins: not all products of the chemical class are active. This suggests specific molecular interactions

rather than unspecific effects such as detergent, hydrophobic, membrane or protein structure disrupting actions.

(2) the mechanism of action is more likely to involve an effect on γ-secretase and/or its micro-environment rather than an interaction with its substrates, as shown by the fact that aftins and triazines also induce a shift in the cleavage pattern of alcadeins, another γ-secretase substrate. The AβPP truncation experiments clearly suggest a very specific molecular requirement rather than a global, non-selective effect.

(3) despite extensive proteomics studies (data not shown), we were unable to detect major/significant modifications of protein expression that might be linked to the AβPP cleavage shift induced by triazines, suggesting that RNA or protein synthesis alterations are unlikely involved in the induction of $A\beta_{42}$ production. We were also unable to identify a specific target of triazines through affinity chromatography/proteomics approaches, suggesting that either the lipid raft comprising the γ-secretase or rather hydrophobic domains of γ-secretase might constitute the real targets of triazines (and aftins).

"Alzheimerogens" in the HCE?

The Chemical Abstracts Service (CAS) registry, the world's largest chemical database, contains more than 101 million organic and non-organic substances. About 15,000 novel substances are registered every day (on average one new substance every 2.5 min. since 50 years!) (www.cas.org). The US EPA Toxic Substances Control Act lists over 84,000 chemicals that are manufactured or imported at levels >10 tons per year, not including pesticides, cosmetics, food stuffs and food additives which are covered by other legislations (www.epa.gov). It is estimated that man is exposed to over 85,000 products. The European REACH initiative aims at regulating all products which are produced/imported at >100 tons/year (>1 ton/year by May 2018). All these products, along with all natural substances to which we are exposed from conception to death, constitute the HCE [17, 18, 48, 49].

The impact of environment on health has been known since antiquity. It is therefore no surprise that a small number of products may enter the human body, cross the blood brain barrier (BBB), alter specific molecular pathways in some of the human brain 10^{11} neurons and 10^{12} glia cells and thereby induce or contribute to specific diseases affecting the central nervous system. Identification of environmental factors involved in neurodegeneration and neurodegenerative diseases is surprisingly still in its infancy [reviews in 50-54]. The nervous system may be exposed to neurotoxic agents acutely (hours, days) or chronically (weeks, years, decades) before disease symptoms appear. Epidemiology studies are particularly

difficult for neurodegenerative diseases since causes and effects are often separated by decades. These studies have, therefore, provided only few examples of environmental agents linked to the onset of neurodegenerative diseases. Pesticides, organic solvents, metals and some natural toxins (cyanobacteria) constitute the most frequently proposed neurotoxic agents. Two recently published books [55, 56] review the impact of early age and even *in utero* exposure to environmental chemical entities on brain development and cognitive abilities.

AD is one of the most prevalent and worrisome neurodegenerative diseases [57]. EOAD is clearly a genetic disease due to specific AβPP or PSEN1/2 mutations leading to overproduction of $A\beta_{42}$ over $A\beta_{40}$. The origin of LOAD (sporadic AD) (>99% of all AD cases) remains a mystery which epidemiological or genome-wide association studies have not solved, the latter having only revealed a few low impact genetic risk factors [58]. The most prominent risk alleles, ApoE ε4 and clusterin/ApoI, link AD to lipid metabolism, and aging, together with several environmental factors, also impose an increased risk. Exposure to numerous industrial and agricultural chemicals correlates with neurotoxicity [50, 51, 52, 53, 54, 59, 60]. Elevated serum pesticides levels, in particular DDE, the major DDT metabolite, are associated with increased risk for AD [61]. DDT increases Aβ levels [61]. There are epidemiological links between exposure to pesticides and AD [63].

Continuous sub-cutaneous injection of aftin-5 in mice triggers robust dose-dependent increase in brain $A\beta_{42}$ levels (unpublished data). Similar results were obtained with aftin-4 [15] and celecoxib or FT-1 [40]. Although orally administered triazines readily cross the BBB, their short half-life in mice prevented any accumulation *in vivo* (data not shown).

Based on results obtained with products belonging to various chemical classes, we can suspect the presence, in the HCE, of products able to increase the production of the AD-associated $A\beta_{42}/A\beta_{43}$ peptides. Such products might be classified as potential "Alzheimerogens" if long-term exposure, slow turn-over, low elimination and BBB permeability allow accumulation in the brain and long-term action on brain cells. It is difficult to predict whether long-term, daily exposures of humans to the widely used triazines described here might have resulted in sustained increase in $A\beta_{42}$ production. We are now investigating other $A\beta_{42}$ inducers which have a longer half-life both in the environment and in man, which accumulate in adipose tissues and which cross the BBB. We believe that such products may contribute to the onset, development and acceleration of sporadic LOAD. It is intriguing that both aftin-5 and triazines were able to stimulate $A\beta_{42}$ production in human cells displaying a pathological AβPP mutation and already showing enhanced $A\beta_{42}$

production. This suggests that environmental factors may synergize with genetic/epigenetic factors in enhancing $A\beta_{42}$ production and triggering AD. Identification of such potential "Alzheimerogens" in the HCE and regulation of human exposure to them should open the way to innovative AD prevention strategies. In addition, some of these products might be turned into pharmacological tools to develop a chemically-induced animal model of AD, with a fundamental and applied potential similar to the MPTP-induced Parkinsonism model [64].

COMPETING INTERESTS

The authors declare that they have no competing interests.

ACKNOWLEDGMENTS

This work was supported by 'Fonds Unique Interministériel' PHARMASEA/TRIAD projects (LM, HG), ANSES (LM, HG) and CRITT-Santé Bretagne /FEDER (LM). This research was also partly supported by an FP7-KBBE-2012 grant (BlueGenics) to LM. MC is CIFRE recipient. KB is a Torsten Söderberg Professor. HZ is a Wallenberg Academy Fellow. This work was supported in part by Grant-in-aid for Scientific Research 26293010 (TS) and 24790062 (SH) from the Ministry of Education, Culture, Sports, Science and Technology in Japan.

REFERENCES

[1] Huang Y, Mucke L (2012) Alzheimer mechanisms and therapeutic strategies. *Cell* **148**, 1204-1222.

[2] Selkoe DJ, Mandelkow E, Holtzman DM (Ed.) (2012) The biology of Alzheimer disease. Cold Spring Harbor Press, Cold Spring Harbor, New York, 511 pp.

[3] Vinters HV (2015) Emerging concepts in Alzheimer's disease. *Annu Rev Pathol* **10**, 291-319.

[4] Bateman RJ, Aisen PS, De Strooper B, Fox NC, Lemere CA, Ringman JM, Salloway S, Sperling RA, Windisch M, Xiong C (2011) Autosomal-dominant Alzheimer's disease a review and proposal for the prevention of Alzheimer's disease. *Alzheimers Res Ther* **3**, 1.

[5] Kuperstein I, Broersen K, Benilova I, Rozenski J, Jonckheere W, Debulpaep M, Vandersteen A, Segers-Nolten I, Van Der Werf K, Subramaniam V, Braeken D, Callewaert G, Bartic C, D'Hooge R, Martins IC, Rousseau F, Schymkowitz J, De

Strooper B (2010) Neurotoxicity of Alzheimer's disease Aβ peptides is induced by small changes in the Aβ42 to Aβ40 ratio. *EMBO J* **29**, 3408-3420.

[6] McGowan E, Pickford F, Kim J, Onstead L, Eriksen J, Yu C, Skipper L, Murphy MP, Beard J, Das P, Jansen K, Delucia M, Lin WL, Dolios G, Wang R, Eckman CB, Dickson DW, Hutton M, Hardy J, Golde T (2005) Abeta42 is essential for parenchymal and vascular amyloid deposition in mice. *Neuron* **47**, 191-199.

[7] Findeis MA (2007) The role of amyloid beta peptide 42 in Alzheimer's disease. *Pharmacol Ther* **116**, 266-286.

[8] Gouras GK, Olsson TT, Hansson O (2014) β-amyloid peptides and amyloid plaques in Alzheimer's disease. *Neurotherapeutics* **12**, 3-11.

[9] Welander H, Frånberg J, Graff C, Sundström E, Winblad B, Tjernberg LO (2009) Abeta43 is more frequent than Abeta40 in amyloid plaque cores from Alzheimer disease brains. *J Neurochem* **110**, 697-706.

[10] Saito T, Suemoto T, Brouwers N, Sleegers K, Funamoto S, Mihira N, Matsuba Y, Yamada K, Nilsson P, Takano J, Nishimura M, Iwata N, Van Broeckhoven C, Ihara Y, Saido TC (2011) Potent amyloidogenicity and pathogenicity of Aβ43. *Nat Neurosci* **14**, 1023-1032.

[11] Sandebring A, Welander H, Winblad B, Graff C, Tjernberg LO (2013) The pathogenic aβ43 is enriched in familial and sporadic Alzheimer disease. *PLoS One* **8**, e55847.

[12] Conicella AE, Fawzi NL (2014) The C-terminal threonine of Aβ43 nucleates toxic aggregation via structural and dynamical changes in monomers and protofibrils. *Biochemistry* **53**, 3095-3105.

[13] Bettayeb K, Oumata N, Zhang Y, Luo W, Bustos V, Galons H, Greengard P, Meijer L, Flajolet M (2012) Small molecule inducers of Aβ42 peptide production share a common mechanism of action. *FASEB J* **26**, 5115-5123.

[14] Hochard A, Oumata N, Bettayeb K, Gloulou O, Fant X, Durieu E, Buron N, Porceddu M, Borgne-Sanchez A, Galons H, Flajolet M, Meijer L (2013) Aftins increase amyloid-β_{42}, lower amyloid-β_{38} and do not alter amyloid-β_{40} in vitro production towards a chemical model of Alzheimer's disease? *J Alzheimers Dis* **35**, 107-120.

[15] Meunier J, Borjini N, Gillis C, Villard V, Maurice T (2015) Brain toxicity and inflammation induced in vivo in mice by the amyloid-β forty-two inducer aftin-4, a roscovitine derivative. *J Alzheimers Dis* **44**, 507-524.

[16] Rappaport SM (2011) Implications of the exposome for exposure science. *J Expo Sci Environ Epidemiol* **21**, 5-9.

[17] Wild CP (2005) Complementing the genome with an "exposome", the outstanding challenge of environmental exposure measurement in molecular epidemiology. *Cancer Epidemiol Biomarkers Prev* **14**, 1847-1850.

[18] Wild CP (2012) The exposome from concept to utility. *Int J Epidemiol* **41**, 24-32.

[19] Juarez PD, Matthews-Juarez P, Hood DB, Im W, Levine RS, Kilbourne BJ, Langston MA, Al-Hamdan MZ, Crosson WL, Estes MG, Estes SM, Agboto VK, Robinson P, Wilson S, Lichtveld MY (2014) The public health exposome a population-based, exposure science approach to health disparities research. *Int J Environ Res Public Health* **11**, 12866-12895.

[20] Vrijheid M, Slama R, Robinson O, Chatzi L, Coen M, van den Hazel P, Thomsen C, Wright J, Athersuch TJ, Avellana N, Basagaña X, Brochot C, Bucchini L, Bustamante M, Carracedo A, Casas M, Estivill X, Fairley L, van Gent D, Gonzalez JR, Granum B, Gražulevičienė R, Gutzkow KB, Julvez J, Keun HC, Kogevinas M, McEachan RR, Meltzer HM, Sabidó E, Schwarze PE, Siroux V, Sunyer J, Want EJ, Zeman F, Nieuwenhuijsen MJ (2014) The human early-life exposome (HELIX), project rationale and design. *Environ Health Perspect* **122**, 535-544.

[21] Wishart D, Arndt D, Pon A, Sajed T, Guo AC, Djoumbou Y, Knox C, Wilson M, Liang Y, Grant J, Liu Y, Goldansaz SA, Rappaport SM (2015) T3DB the toxic exposome database. *Nucleic Acids Res* **43**, D928-934.

[22] Portelius E, Price E, Brinkmalm G, Stiteler M, Olsson M, Persson R, Westman-Brinkmalm A, Zetterberg H, Simon AJ, Blennow K (2011) A novel pathway for amyloid precursor protein processing. *Neurobiol Aging* **32**, 1090-1098.

[23] Pérez-Grijalba V, Pesini P, Allué JA, Sarasa L, Montañés M, Lacosta AM, Casabona D, San-José I, Boada M, Tárraga L, Ruiz A, Sarasa M (2015) Aβ1-17 is a major amyloid-β fragment isoform in cerebrospinal fluid and blood with possible diagnostic value in Alzheimer's disease. *J Alzheimers Dis* **43**, 47-56.

[24] Araki Y, Kawano T, Taru H, Saito Y, Wada S, Miyamoto K, Kobayashi H, Ishikawa HO, Ohsugi Y, Yamamoto T, Matsuno K, Kinjo M, Suzuki T (2007) The novel cargo Alcadein induces vesicle association of kinesin-1 motor components and activates axonal transport. *EMBO J* **26**, 1475-1486.

[25] Hata S, Fujishige S, Araki Y, Kato N, Araseki M, Nishimura M, Hartmann D, Saftig P, Fahrenholz F, Taniguchi M, Urakami K, Akatsu H, Martins RN, Yamamoto K, Maeda M, Yamamoto T, Nakaya T, Gandy S, Suzuki T (2009) Alcadein cleavages by amyloid beta-precursor protein (APP) alpha- and gamma-secretases generate small peptides, p3-

Alcs, indicating Alzheimer disease-related gamma-secretase dysfunction. *J Biol Chem* **284**, 36024-36033.

[26] Kamogawa K, Kohara K, Tabara Y, Takita R, Miki T, Konno T, Hata S, Suzuki T (2012) Potential utility of soluble p3-alcadein α plasma levels as a biomarker for sporadic Alzheimer's disease. *J Alzheimers Dis* **31**, 421-428.

[27] Piao Y, Kimura A, Urano S, Saito Y, Taru H, Yamamoto T, Hata S, Suzuki T (2013) Mechanism of intramembrane cleavage of alcadeins by γ-secretase. *PLoS One* **8**, e62431.

[28] Omori C, Kaneko M, Nakajima E, Akatsu H, Waragai M, Maeda M, Morishima-Kawashima M, Saito Y, Nakaya T, Taru H, Yamamoto T, Asada T, Hata S, Suzuki T; Japanese Alzheimer's Disease Neuroimaging Initiative (2014) Increased levels of plasma p3-alcα35, a major fragment of Alcadeinα by γ-secretase cleavage, in Alzheimer's disease. *J Alzheimers Dis* **39**, 861-870.

[29] Lebaron H.M., McFarland J.E., Burnside O.C. (Ed.) (2008) The triazine herbicides. Elsevier, Amsterdam, 584 pp.

[30] Kounnas MZ, Danks AM, Cheng S, Tyree C, Ackerman E, Zhang X, Ahn K, Nguyen P, Comer D, Mao L, Yu C, Pleynet D, Digregorio PJ, Velicelebi G, Stauderman KA, Comer WT, Mobley WC, Li YM, Sisodia SS, Tanzi RE, Wagner SL (2010) Modulation of gamma-secretase reduces beta-amyloid deposition in a transgenic mouse model of Alzheimer's disease. *Neuron* **67**, 769-780.

[31] Kretner B, Fukumori A, Gutsmiedl A, Page RM, Luebbers T, Galley G, Baumann K, Haass C, Steiner H (2011) Attenuated Abeta42 responses to low potency gamma-secretase modulators can be overcome for many pathogenic presenilin mutants by second-generation compounds. *J Biol Chem* **286**, 15240-15251.

[32] Ahn YH, Chang YT (2007) Tagged small molecule library approach for facilitated chemical genetics. *Acc Chem Res* **40**, 1025-1033.

[33] Lee JW, Bork JT, Ha HH, Samanta A, Chang YT (2009) Novel orthogonal synthesis of a tagged combinatorial triazine library via Grignard reaction. *Aust J Chem* **62**, 1000-1006.

[34] Leinenbach A., Pannee J, Dülffer T, Huber A, Bittner T, Andreasson U, Gobom J, Zetterberg H, Kobold U, Portelius E, Blennow K; IFCC Scientific Division Working Group on CSF proteins (2014) Mass spectrometry-based candidate reference measurement procedure for quantification of amyloid-β in cerebrospinal fluid. *Clin Chem* **60**, 987-994.

[35] Pannee J, Portelius E, Oppermann M, Atkins A, Hornshaw M, Zegers I, Höjrup P, Minthon L, Hansson O, Zetterberg H, Blennow K, Gobom J (2013) A selected reaction monitoring (SRM)-based method for absolute quantification of Aβ-38, Aβ-40, and Aβ42 in cerebrospinal fluid of Alzheimer's disease patients and healthy controls. *J Alzheimers Dis* **33**, 1021-1032.

[36] Portelius E, Olsson M, Brinkmalm G, Rüetschi U, Mattsson N, Andreasson U, Gobom J, Brinkmalm A, Hölttä M, Blennow K, Zetterberg H (2013) Mass spectrometric characterization of amyloid-β species in the 7PA2 cell model of Alzheimer's disease. *J Alzheimers Dis* **33**, 85-93.

[37] Mertens J, Stüber K, Wunderlich P, Ladewig J, Kesavan JC, Vandenberghe R, Vandenbulcke M, van Damme P, Walter J, Brüstle O, Koch P (2013) APP processing in human pluripotent stem cell-derived neurons is resistant to NSAID-based γ-secretase modulation. *Stem Cell Reports* **1**, 491-498.

[38] Koch P., Tamboli IY, Mertens J, Wunderlich P, Ladewig J, Stüber K, Esselmann H, Wiltfang J, Brüstle O, Walter J (2012) Presenilin-1 L166P mutant human pluripotent stem cell-derived neurons exhibit partial loss of γ-secretase activity in endogenous amyloid-β generation. *Am J Pathol* **180**, 2404-2416.

[39] Koch P, Opitz T, Steinbeck JA, Ladewig J, Brüstle O (2009) A rosette-type, self-renewing human ES cell-derived neural stem cell with potential for in vitro instruction and synaptic integration. *Proc Natl Acad Sci USA* **106**, 3225-3230.

[40] Kukar T, Murphy MP, Eriksen JL, Sagi SA, Weggen S, Smith TE, Ladd T, Khan MA, Kache R, Beard J, Dodson M, Merit S, Ozols VV, Anastasiadis PZ, Das P, Fauq A, Koo EH, Golde TE (2005) Diverse compounds mimic Alzheimer disease-causing mutations by augmenting Abeta42 production. *Nat Med* **11**, 545-550.

[41] Svedružić ŽM, Popović K, Šendula-Jengić V (2013) Modulators of γ-secretase activity can facilitate the toxic side-effects and pathogenesis of Alzheimer's disease. *PLoS One* **8**, e50759.

[42] Barnwell E, Padmaraju V, Baranello R, Pacheco-Quinto J, Crosson C, Ablonczy Z, Eckman E, Eckman CB, Ramakrishnan V, Greig NH, Pappolla MA, Sambamurti K (2014) Evidence of a novel mechanism for partial γ-secretase inhibition induced paradoxical increase in secreted amyloid β protein. *PLoS One* **9**, e91531.

[43] Jung JI, Ladd TB, Kukar T, Price AR, Moore BD, Koo EH, Golde TE, Felsenstein KM (2013) Steroids as γ-secretase modulators. *FASEB J* **27**, 3775-3785.

[44] Takasugi N, Sasaki T, Shinohara M, Iwatsubo T, Tomita T (2015) Synthetic ceramide analogues increase amyloid-β 42 production by modulating γ-secretase activity. *Biochem Biophys Res Commun* **457**, 194-199.

[45] Guix FX, Wahle T, Vennekens K, Snellinx A, Chávez-Gutiérrez L, Ill-Raga G, Ramos-Fernandez E, Guardia-Laguarta C, Lleó A, Arimon M, Berezovska O, Muñoz FJ, Dotti CG, De Strooper B (2012) Modification of γ-secretase by nitrosative stress links neuronal ageing to sporadic Alzheimer's disease. *EMBO Mol Med* **4**, 660-673.

[46] Portelius E, Andreasson U, Ringman JM, Buerger K, Daborg J, Buchhave P, Hansson O, Harmsen A, Gustavsson MK, Hanse E, Galasko D, Hampel H, Blennow K, Zetterberg H (2010) Distinct cerebrospinal fluid amyloid beta peptide signatures in sporadic and PSEN1 A431E-associated familial Alzheimer's disease. *Mol Neurodegener* **5**, 2.

[47] Portelius E, Fortea J, Molinuevo JL, Gustavsson MK, Andreasson U, Sanchez-Valle R (2012) The amyloid-beta isoform pattern in cerebrospinal fluid in familial PSEN1 M139T- and L286P-associated Alzheimer's disease. *Mol Med Rep* **5**, 1111-1115.

[48] Egeghy PP, Judson R, Gangwal S, Mosher S, Smith D, Vail J, Cohen Hubal EA (2012) The exposure data landscape for manufactured chemicals. *Sci Total Environ* **414**, 159-166.

[49] Goldsmith MR, Grulke CM, Brooks RD, Transue TR, Tan YM, Frame A, Egeghy PP, Edwards R, Chang DT, Tornero-Velez R, Isaacs K, Wang A, Johnson J, Holm K, Reich M, Mitchell J, Vallero DA, Phillips L, Phillips M, Wambaugh JF, Judson RS, Buckley TJ, Dary CC (2014) Development of a consumer product ingredient database for chemical exposure screening and prioritization. *Food Chem Toxicol* **65**, 269- 279.

[50] Grandjean P, Landrigan P.J. (2006) Developmental neurotoxicity of industrial chemicals. *Lancet* **368**, 2167-2178.

[51] Grandjean P, Landrigan PJ (2014) Neurobehavioural effects of developmental toxicity. *Lancet Neurol* **13**, 330-338.

[52] Cannon JR, Greenamyre JT (2011) The role of environmental exposures in neurodegeneration and neurodegenerative diseases. *Toxicol Sci* **124**, 225-250.

[53] Chin-Chan M, Navarro-Yepes J, Quintianilla-Vega B (2015) Environmental pollutants as risk factors for neurodegenerative disorders: Alzheimer and Parkinson diseases. *Frontiers Cell Neurosci* **9**, 124.

[54] Yegambaram M, Manivannan B, Beach TG, Halden RU (2015) Role of environmental contaminants in the etiology of Alzheimer's disease: a review. *Curr Alzheimer Res* **12**, 116-146.

[55] Grandjean P (2013) Only one chance. How environmental pollution impairs brain development - and how to protect the brains of the next generation. Oxford University Press, 212 pp.

[56] Demeneix B (2014) Losing our minds. How environmental pollution impairs human intelligence and mental health. Oxford University Press, 284 pp.

[57] Alzheimer's Association Alzheimer's disease facts and figures. (2015) *Alzheimers Dement* **11**, 332-384.

[58] Lambert JC, Ibrahim-Verbaas CA, Harold D, Naj AC, Sims R, Bellenguez C, DeStafano AL, Bis JC, Beecham GW, Grenier-Boley B, Russo G, Thorton-Wells TA, Jones N, Smith AV, Chouraki V, Thomas C, Ikram MA, Zelenika D, Vardarajan BN, Kamatani Y, Lin CF, Gerrish A, Schmidt H, Kunkle B, Dunstan ML, Ruiz A, Bihoreau MT, Choi SH, Reitz C, Pasquier F, Cruchaga C, Craig D, Amin N, Berr C, Lopez OL, De Jager PL, Deramecourt V, Johnston JA, Evans D, Lovestone S, Letenneur L, Morón FJ, Rubinsztein DC, Eiriksdottir G, Sleegers K, Goate AM, Fiévet N, Huentelman MW, Gill M, Brown K, Kamboh MI, Keller L, Barberger-Gateau P, McGuiness B, Larson EB, Green R, Myers AJ, Dufouil C, Todd S, Wallon D, Love S, Rogaeva E, Gallacher J, St George-Hyslop P, Clarimon J, Lleo A, Bayer A, Tsuang DW, Yu L, Tsolaki M, Bossù P, Spalletta G, Proitsi P, Collinge J, Sorbi S, Sanchez-Garcia F, Fox NC, Hardy J, Deniz Naranjo MC, Bosco P, Clarke R, Brayne C, Galimberti D, Mancuso M, Matthews F; European Alzheimer's Disease Initiative (EADI); Genetic and Environmental Risk in Alzheimer's Disease; Alzheimer's Disease Genetic Consortium; Cohorts for Heart and Aging Research in Genomic Epidemiology, Moebus S, Mecocci P, Del Zompo M, Maier W, Hampel H, Pilotto A, Bullido M, Panza F, Caffarra P, Nacmias B, Gilbert JR, Mayhaus M, Lannefelt L, Hakonarson H, Pichler S, Carrasquillo MM, Ingelsson M, Beekly D, Alvarez V, Zou F, Valladares O, Younkin SG, Coto E, Hamilton-Nelson KL, Gu W, Razquin C, Pastor P, Mateo I, Owen MJ, Faber KM, Jonsson PV, Combarros O, O'Donovan MC, Cantwell LB, Soininen H, Blacker D, Mead S, Mosley TH Jr, Bennett DA, Harris TB, Fratiglioni L, Holmes C, de Bruijn RF, Passmore P, Montine TJ, Bettens K, Rotter JI, Brice A, Morgan K, Foroud TM, Kukull WA, Hannequin D, Powell JF, Nalls MA, Ritchie K, Lunetta KL, Kauwe JS, Boerwinkle E, Riemenschneider M, Boada M, Hiltuenen M, Martin ER, Schmidt R, Rujescu D, Wang LS, Dartigues JF, Mayeux R, Tzourio C, Hofman A, Nöthen MM, Graff C, Psaty BM, Jones L, Haines JL, Holmans PA, Lathrop M, Pericak-Vance MA, Launer LJ, Farrer LA, van Duijn CM, Van Broeckhoven C, Moskvina V, Seshadri S, Williams J,

Schellenberg GD, Amouyel P (2013) Meta-analysis of 74,046 individuals identifies 11 new susceptibility loci for Alzheimer's disease. *Nat Genet* **45**, 1452-1458.

[59] Julvez J, Grandjean P (2009) Neurodevelopmental toxicity risks due to occupational exposure to industrial chemicals during pregnancy. *Ind Health* **47**, 459-468.

[60] Zeliger HI (2013) Exposure to lipophilic chemicals as a cause of neurological impairments, neurodevelopmental disorders and neurodegenerative diseases. *Interdiscipl Toxicol* **6**, 103-110.

[61] Richardson JR, Roy A, Shalat SL, von Stein RT, Hossain MM, Buckley B, Gearing M, Levey AI, German DC (2014) Elevated serum pesticide levels and risk for Alzheimer disease. *JAMA Neurol* **71**, 284-290.

[62] Li G, Kim C, Kim J, Yoon H, Zhou H, Kim J (2015) Common pesticide, dichlorodiphenyltrichloroethane (DDT), increases amyloid-β levels by impairing the function of ABCA1 and IDE implication for Alzheimer's disease. *J Alzheimers Dis* **46**, 109-122.

[63] Hayden KM, Norton MC, Darcey D, Ostbye T, Zandi PP, Breitner JC, Welsh-Bohmer KA, Cache County Study Investigators (2010) Occupational exposure to pesticides increases the risk of incident AD the Cache County study. *Neurology* **74**, 1524-1530.

[64] Fox SH, Brotchie JM (2010) The MPTP-lesioned non-human primate models of Parkinson's disease. Past, present, and future. *Prog Brain Res* **184**, 133-157.

[65] Banker G, Goslin K (1988) Developments in neuronal cell culture. *Nature* **336**, 185-186

[66] Mehta PD, Pirttila T (2005) Increased cerebrospinal fluid A beta38/A beta42 ratio in Alzheimer disease. *Neurodegener Dis* **2**, 242-245.

[67] Potempska A, Mack K, Mehta P, Kim KS, Miller DL (1999) Quantification of sub-femtomole amounts of Alzheimer amyloid beta peptides. *Amyloid* **6**, 14-21.

[68] Portelius E, Tran AJ, Andreasson U, Persson R, Brinkmalm G, Zetterberg H, Blennow K, Westman-Brinkmalm A (2007) Characterization of amyloid beta peptides in cerebrospinal fluid by an automated immunoprecipitation procedure followed by mass spectrometry. *J Proteome Res* **6**, 4433-4439.

FIGURE LEGENDS

Fig. 1. Some triazines trigger β- and γ-secretase dependent production of extracellular Aβ42. A. Effect of 37 triazines on extracellular Aβ42 production by N2a-APP695 and CHO-7PA2-APPsw cells. Cells were treated with 100 μM of each compound for 18 h and cell supernatants were collected for Aβ42 levels measurement by ELISA. Aftin-5 was used as a positive control and the corresponding volume of DMSO as a negative control. Levels are expressed as fold change, average ± SEM of triplicate values, of Aβ42 levels over those of control, vehicle-treated cells.(representative of four independent experiments). Horizontal dotted lines indicate levels for 1 and 3 fold changes in Aβ42 concentration. **B.** Structure of the six active triazines and of aftin-5. **C.** Extracellular Aβ42 production induced by triazines is inhibited by β-secretase inhibitor IV, γ-secretase inhibitors DAPT & BMS 299897 and γ-secretase modulator 'Torrey Pines' compound. N2a-APP695 cells were exposed to 10 μM of each inhibitor. 1.5 h later, cells were treated with 100 μM of each active triazine or 50 μM aftin-5. Extracellular Aβ42 levels were measured after 18 h. Average ± SEM of triplicate values (representative of two independent experiments). **D.** Triazines trigger Aβ42 production in primary rat neuron cultures. Cells were exposed to DMSO, 100 μM of each triazine or aftin-5 for 18 h. Cell supernatants were collected and the levels of Aβ38, Aβ40 and Aβ42 (bottom panel) were determined by ELISA assays (average ± SEM of triplicate values). The Aβ42/Aβ40 ratios are shown in the top panel. The horizontal dotted line refers to the basal ratio in control cells.

Fig. 2. Absolute quantification of Aβ38, Aβ40 and Aβ42 using LC-MS/MS. Levels of the three amyloid peptides were determined by mass spectrometry in supernatants of N2a-APP695 (**A**) and CHO-7PA2-APPsw (**B**) cells following 18 h treatment with DMSO, 100 μM of each triazine or aftin-5. Amyloid levels are expressed as percentage of levels in vehicle-treated cells (bottom panels; average ± SEM of triplicate values; absolute values in control cell supernatants are indicated under the bottom panels). Aβ42/Aβ40 ratios are shown in the top panels (horizontal dotted lines refer to the basal ratios in control cells).

Fig. 3. Pattern of amyloid peptides produced by CHO-7PA2-APPsw cells exposed to triazines. Cells were treated for 18 h with DMSO, 100 μM of each triazine or aftin-5. Cell supernatants were collected and analyzed as described. **A**. Example spectra of supernatants amyloid profiles from CHO-7PA2-APPsw cells exposed to DMSO, aftin-5 or terbutryn. **B**.

Quantification of all amyloid peptides in CHO-7PA2-APPsw cell supernatants (Log of fold change in triazine or aftin-5 treated cells over control, DMSO-treated cells).

Fig. 4. Triazines trigger enhanced production of Aβ42 versus Aβ40 in neurons differentiated from human iPSCs. A. iPSCs-derived neurons were differentiated for 4 or 10 weeks and then exposed to DMSO or 100 μM aftin-5 or terbutryn (**14**) for 24 h. **B.** Neurons were derived from iPSCs obtained from a healthy donor (AβPP WT) or from an AD patient (AβPP K724N mutation). They were exposed for 24 h to DMSO, 100 μM aftin-5 or the six triazines. In both experiments cell supernatants were collected for extracellular Aβ levels measurement. Levels are expressed as $A\beta_{42}/A\beta_{40}$ ratios ± SEM of triplicate values.

Fig. 5. Effect of AβPP C-terminal truncations on triazines' efficacy. A. Only the C-terminal aa sequences of AβPP full length (WT) and C-terminal truncations mutants (T1-T6) are shown. The γ and ε cleavage sites are indicated in orange and blue respectively. Numbers indicate the position of the residues involved in those cleavages and refer to the α cleavage site. **B**. Mutants T1 to T6 were expressed transiently in N2a cells which were exposed to DMSO or aftin-5 (100 μM) for 24 h and the levels of released $A\beta_{42}$ was measured by ELISA (average ± SEM of triplicate values). **C**. Mutants T1, T3 and T4 expressing N2a cells were exposed for 24 h to DMSO (D), aftin-5 or the six triazines (100 μM). $A\beta_{42}$ level were measured and are expressed as fold-increase vs. untreated cells (average ± SEM of triplicate values).

Fig. 6. Triazines alter the cleavage pattern of Alcadeinα, leading to increased p3-Alcα38 production. A. Schematic representation of the production of p3-Alcα peptides from Alcadeinα. The full length protein is cleaved primarily by α-secretase at His814 or Ala816 (purple arrows). It is then cleaved by γ-secretase at Thr851 (orange arrow) leading to the two main Alcadeinα peptides p3-Alcα35 and p3-Alcα2N+35 ('2N' denotes the two additional, N-terminal amino acids). Alternative cleavage sites (blue arrows) generate additional p3-Alcα peptides of different sizes. **B**. Immunoprecipitation/mass spectrometry spectra of p3-Alcα peptides produced by HEK-Alcadein α cells exposed to various triazines, aftin-5 or DMSO. Cells were treated for 24 h with 100 μM of each reagent and p3-Alc peptides were analyzed by MALDI-TOF/MS. Representative profiles for each product (top) and zoom on the p3-Alcα2N+34, p3-Alcα2N+35 and p3-Alcα2N+38 peaks (bottom). **C**. Relative quantification of p3-Alcα peptides produced by cells exposed to all triazines and aftin-5. Levels of each peptide

are presented as fold change of ratios over p3-Alcα2N+35 versus corresponding peptide ratios for DMSO-treated cells (average ± SEM of triplicate values). Horizontal dotted lines indicate levels for 1 fold change in p3-Alcα/p3-Alcα35 ratio in treated vs. control cell supernatant. Note the change of scale for p3-Alcα2N+38/p3-Alcα2N+35 treated/control ratio.

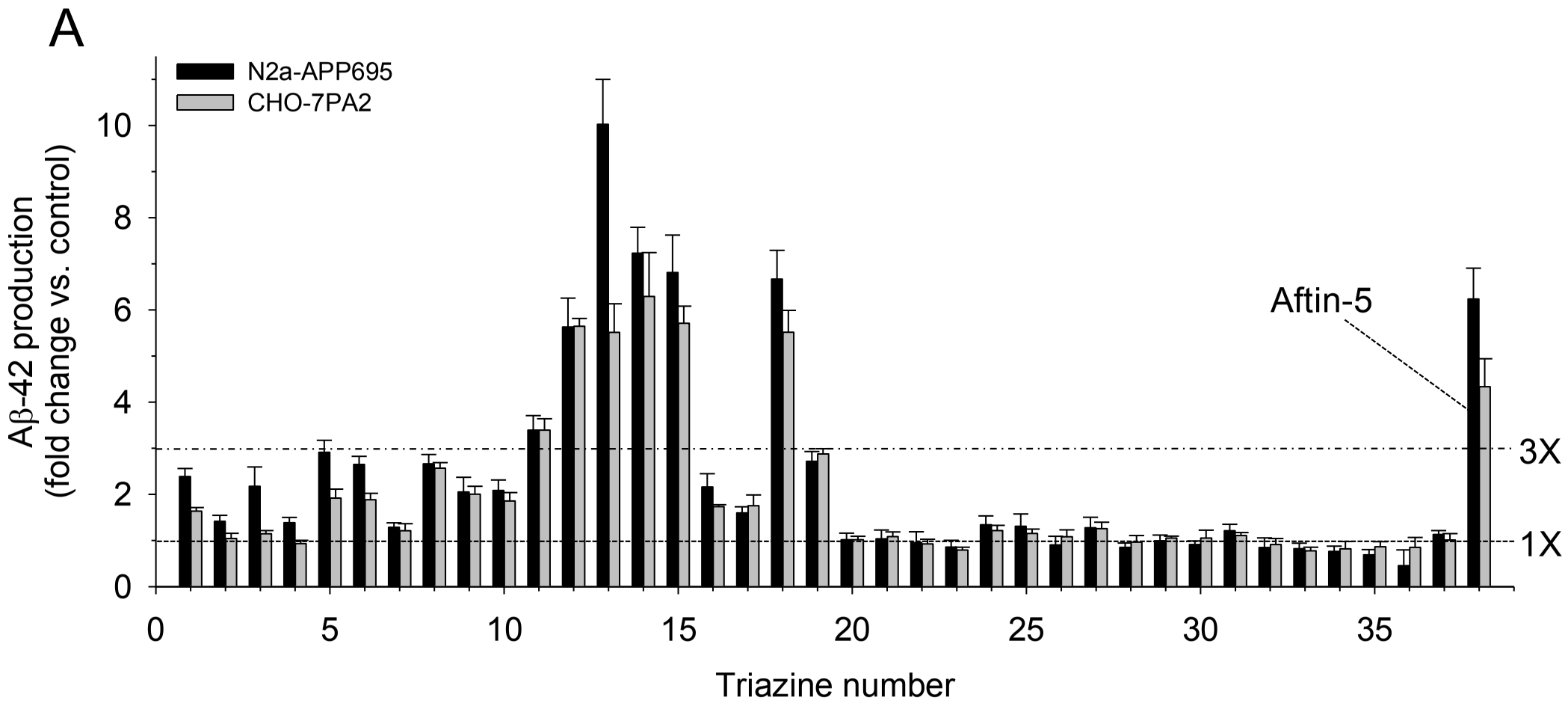

Portelius et al. Figure 1A

B

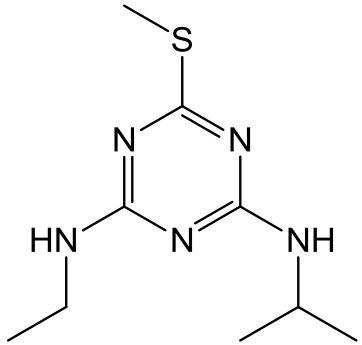

Ametryn (**11**)

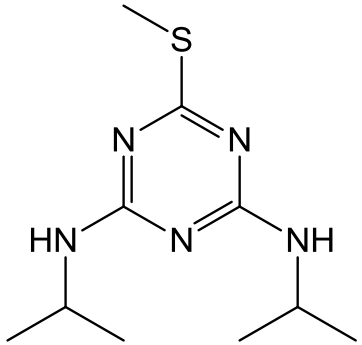

Prometryn (**12**)

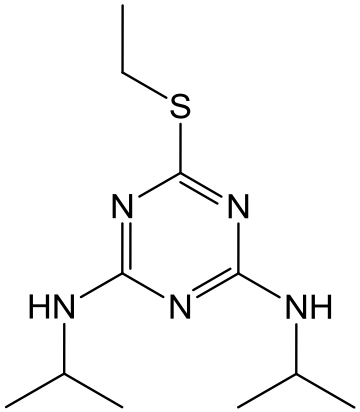

Dipropetryn (**13**)

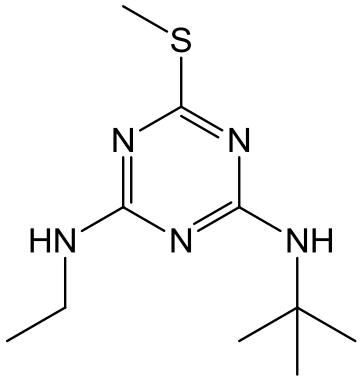

Terbutryn (**14**)

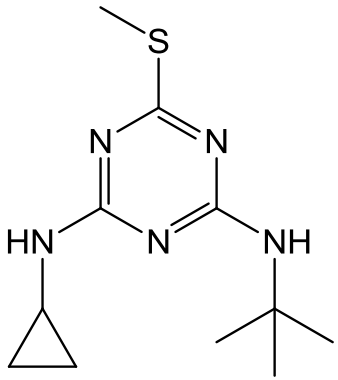

Cybutryne (**15**)

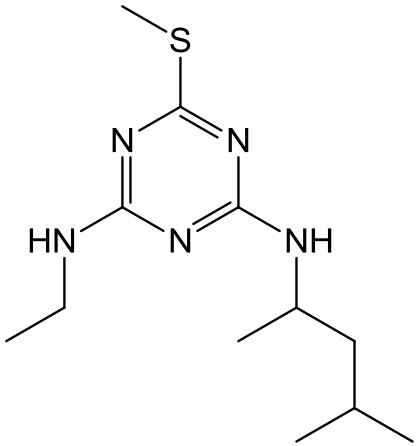

Dimethametryn (**18**)

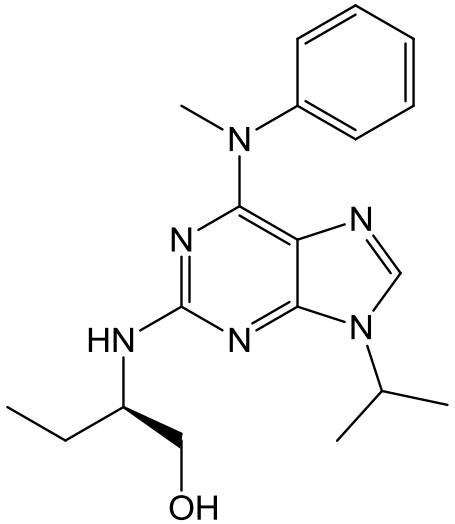

Aftin-5 (**38**)

Portelius et al. Figure 1B

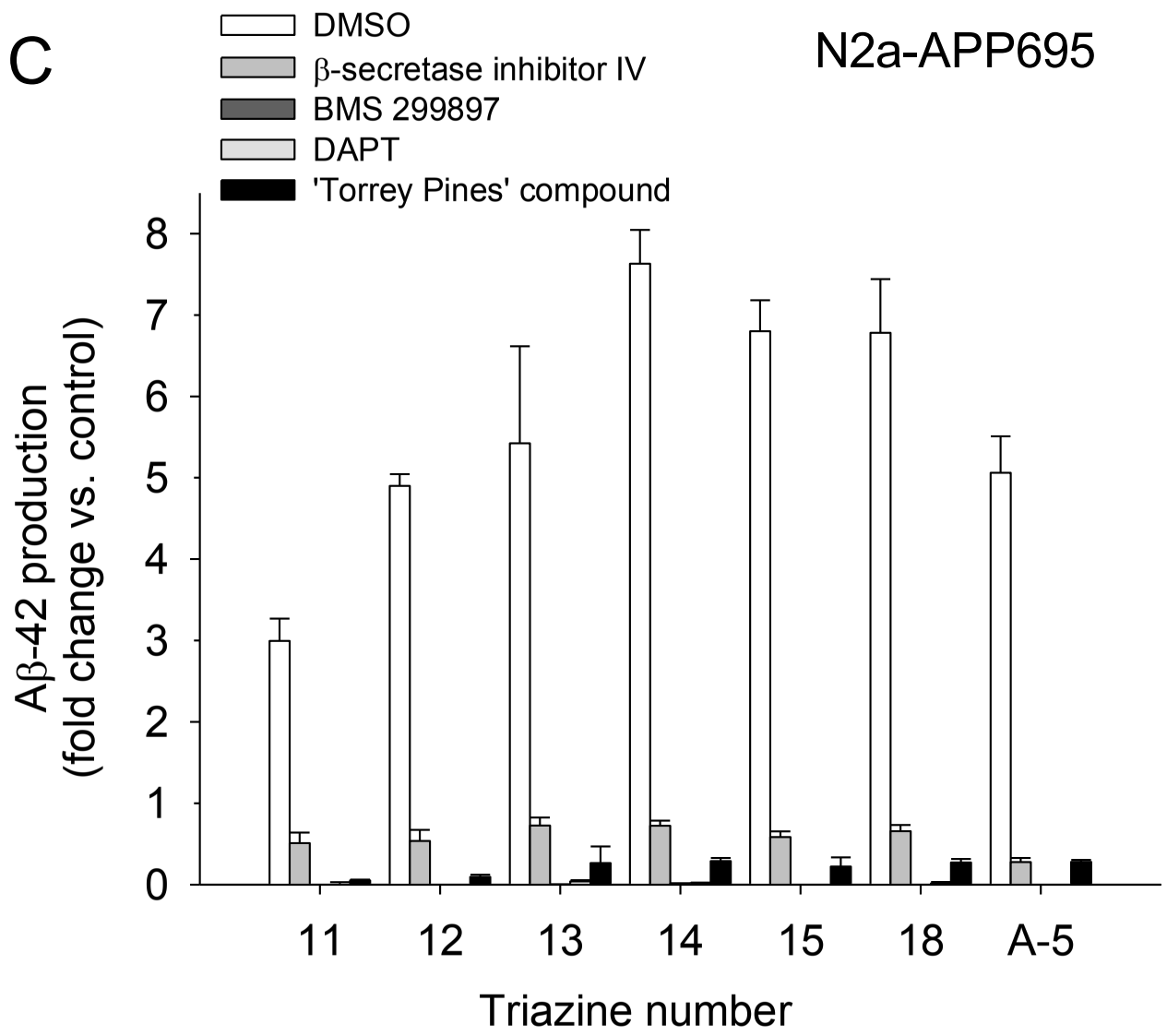

Portelius et al. Figure 1C

D

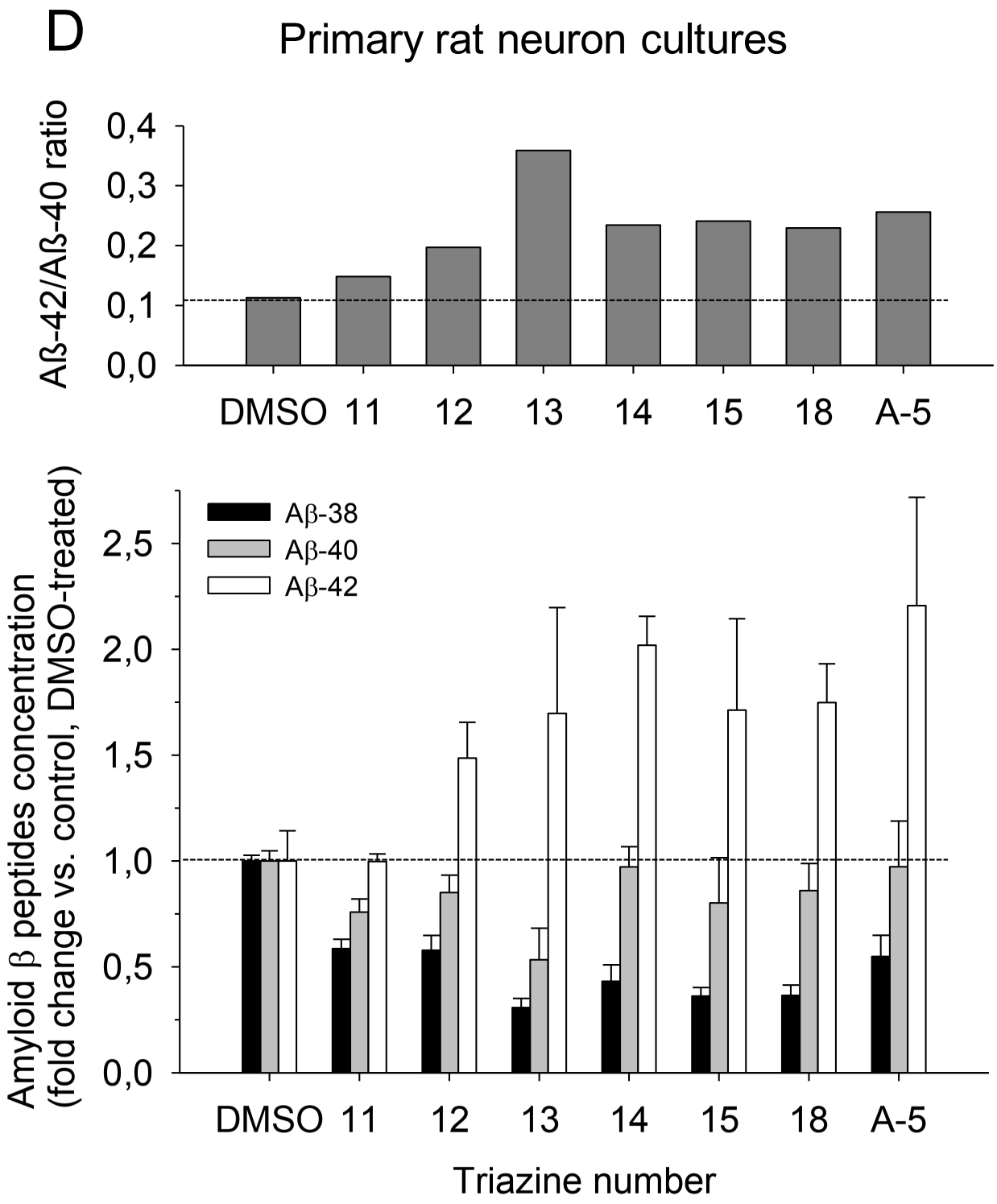

Portelius et al. Figure 1D

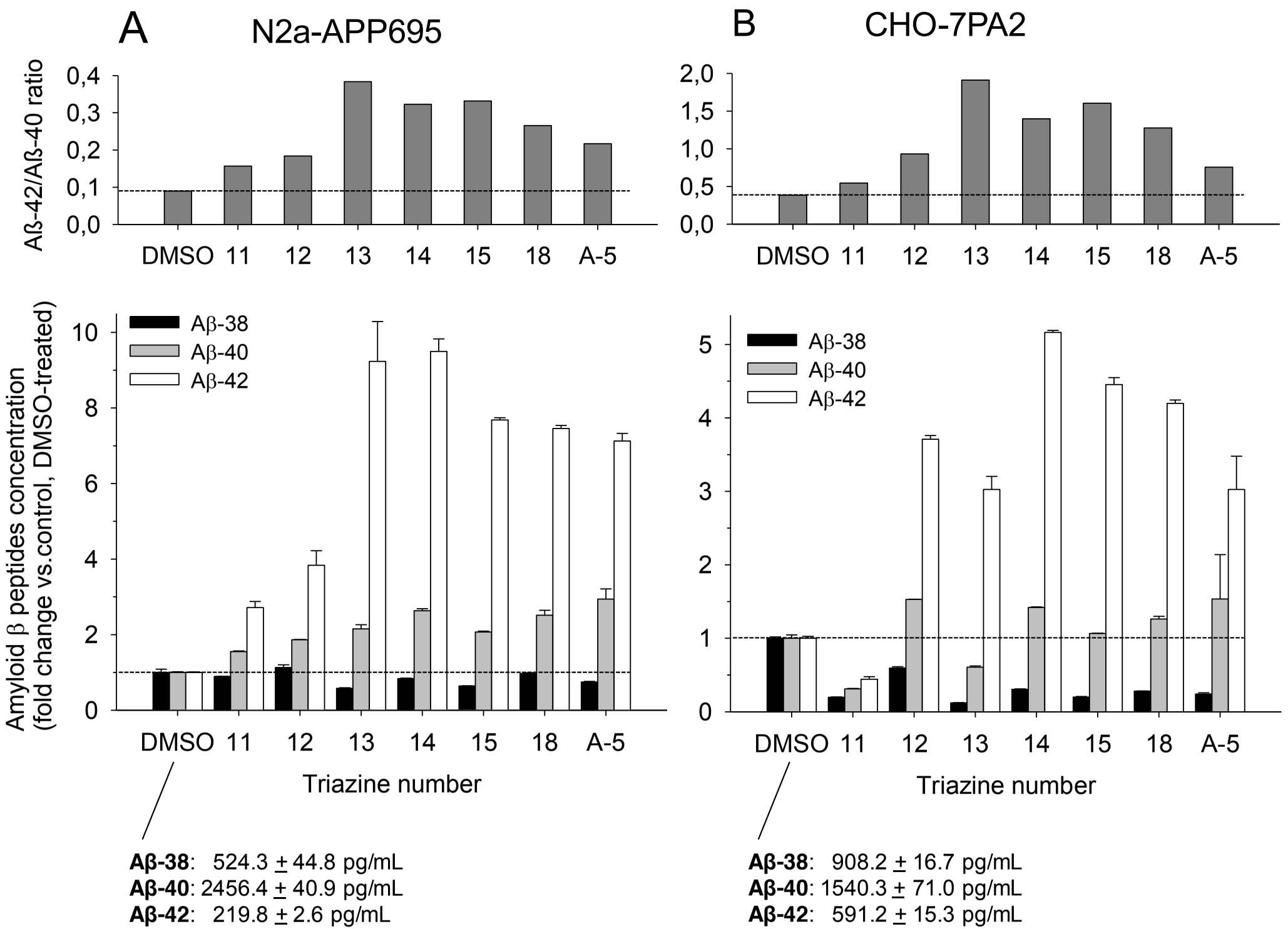

Aβ-38: 524.3 ± 44.8 pg/mL
Aβ-40: 2456.4 ± 40.9 pg/mL
Aβ-42: 219.8 ± 2.6 pg/mL

Aβ-38: 908.2 ± 16.7 pg/mL
Aβ-40: 1540.3 ± 71.0 pg/mL
Aβ-42: 591.2 ± 15.3 pg/mL

Portelius et al. Figure 2

A CHO-7PA2

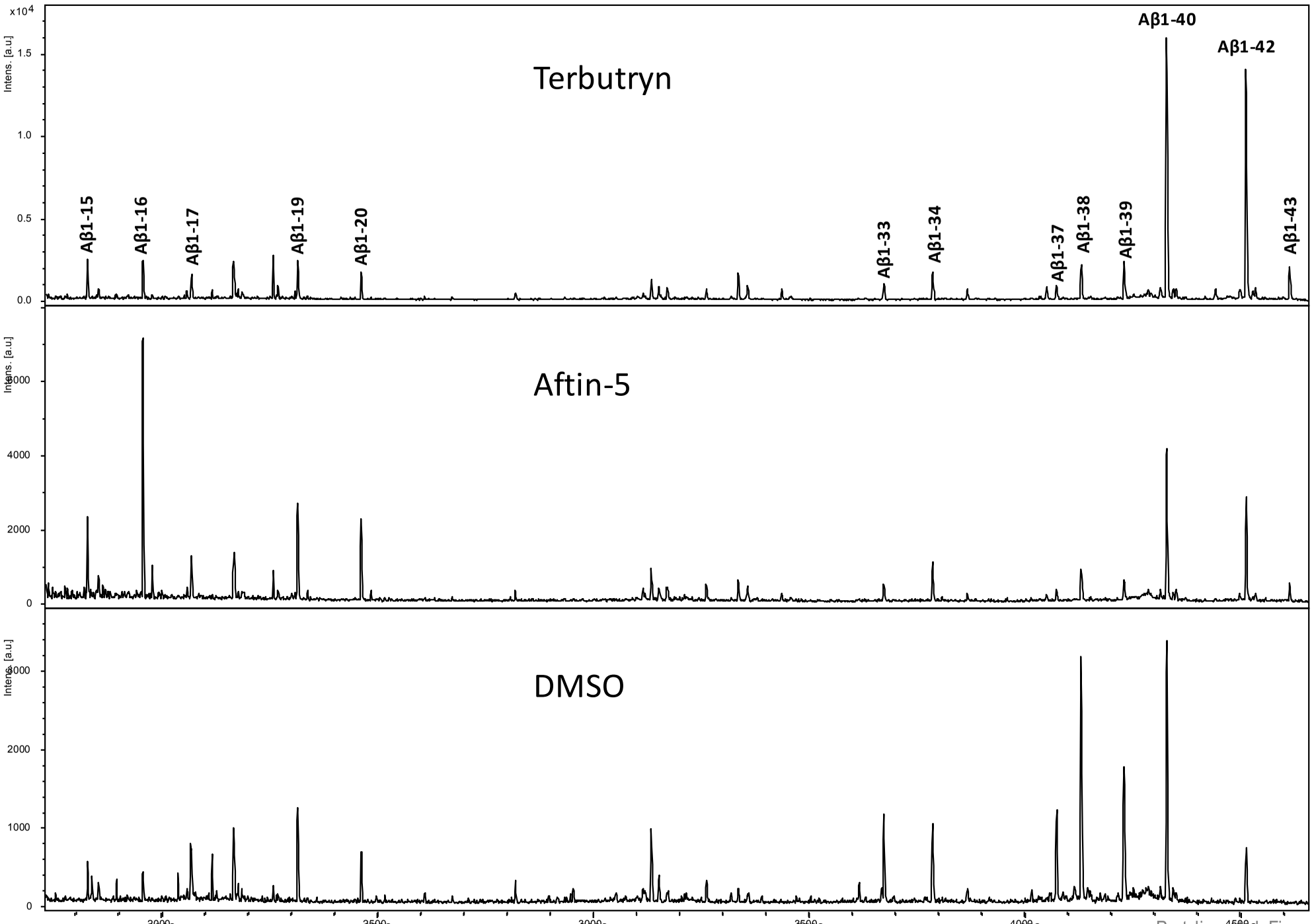

Portelius et al. Figure 3C

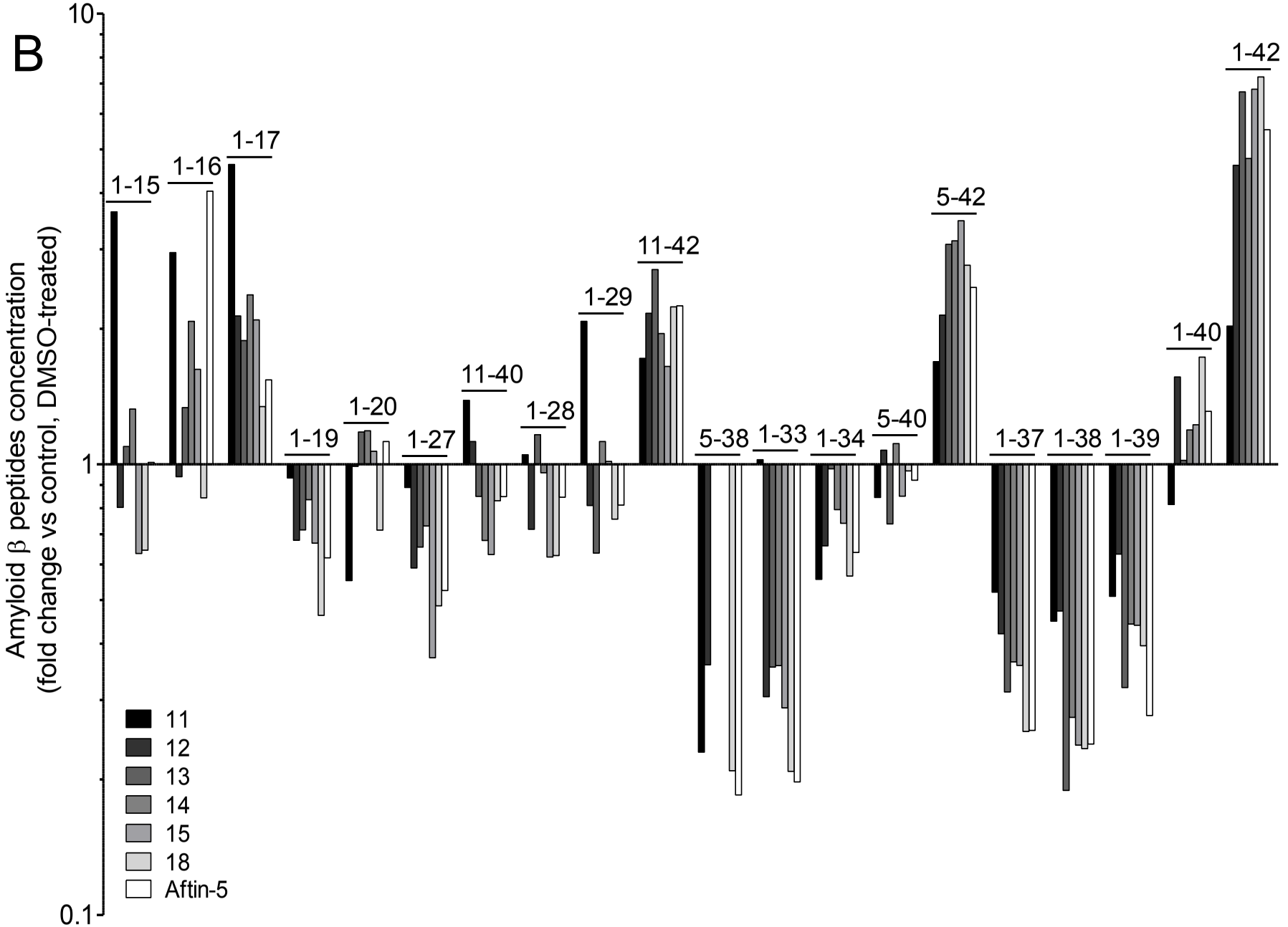

Portelius et al. Figure 3D

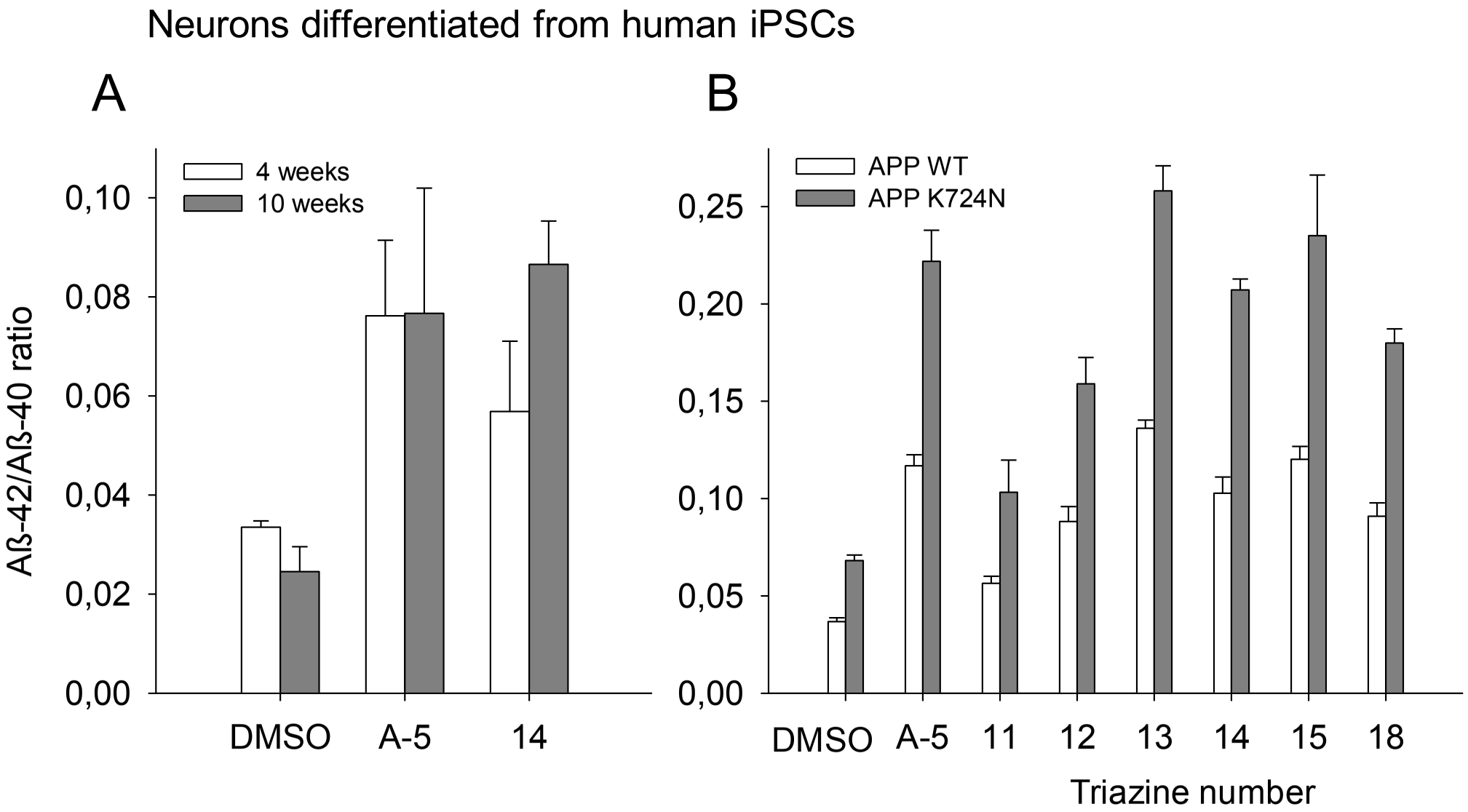

Portelius et al. Figure 4

Portelius et al. Figure 5A

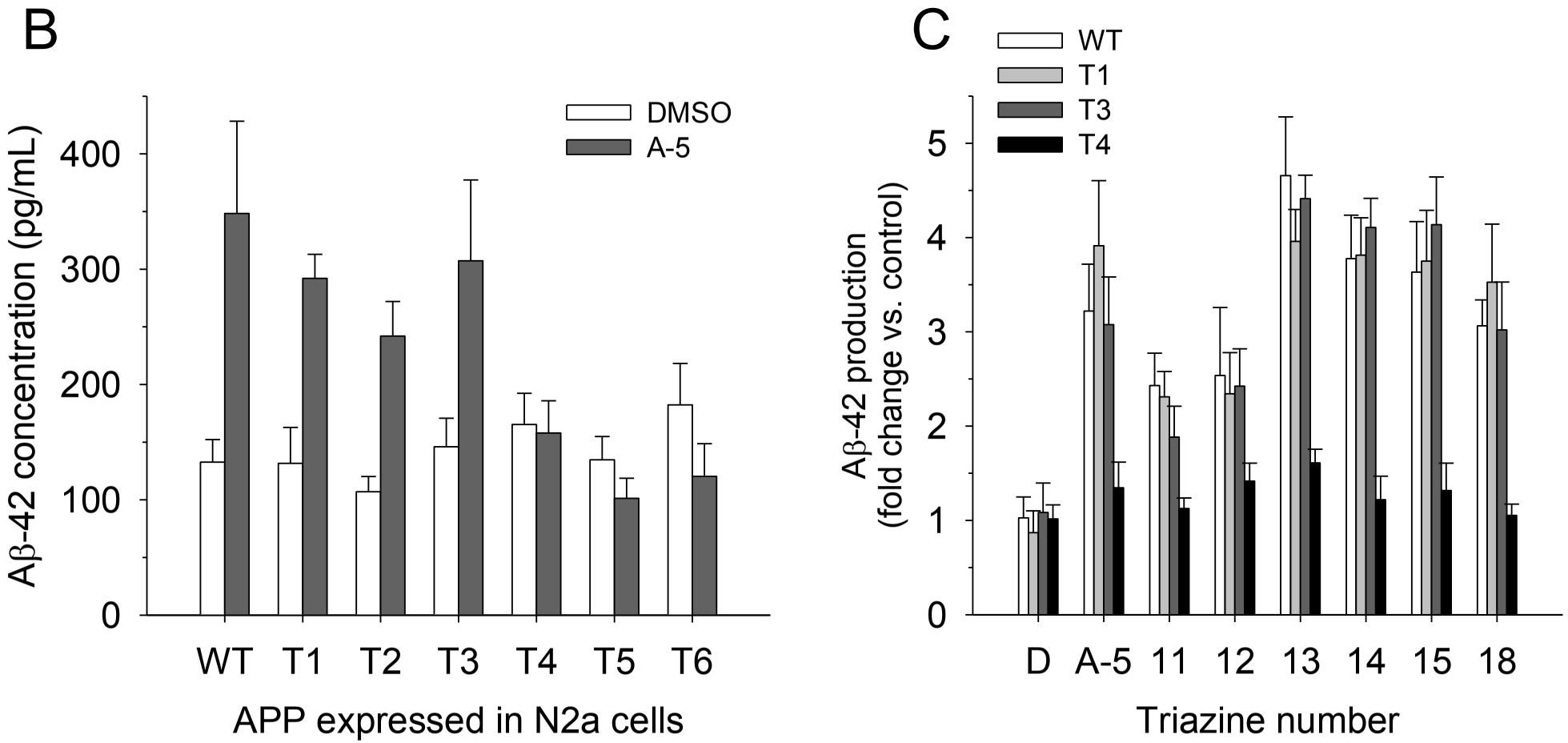

Portelius et al. Figure 5B, C

A

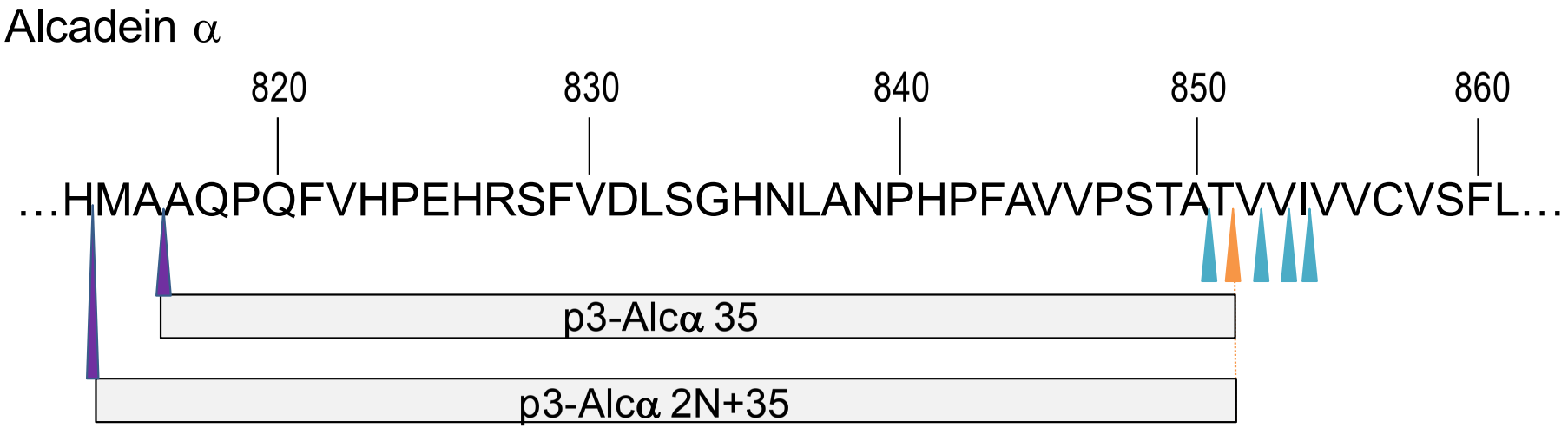

Portelius et al. Figure 6A

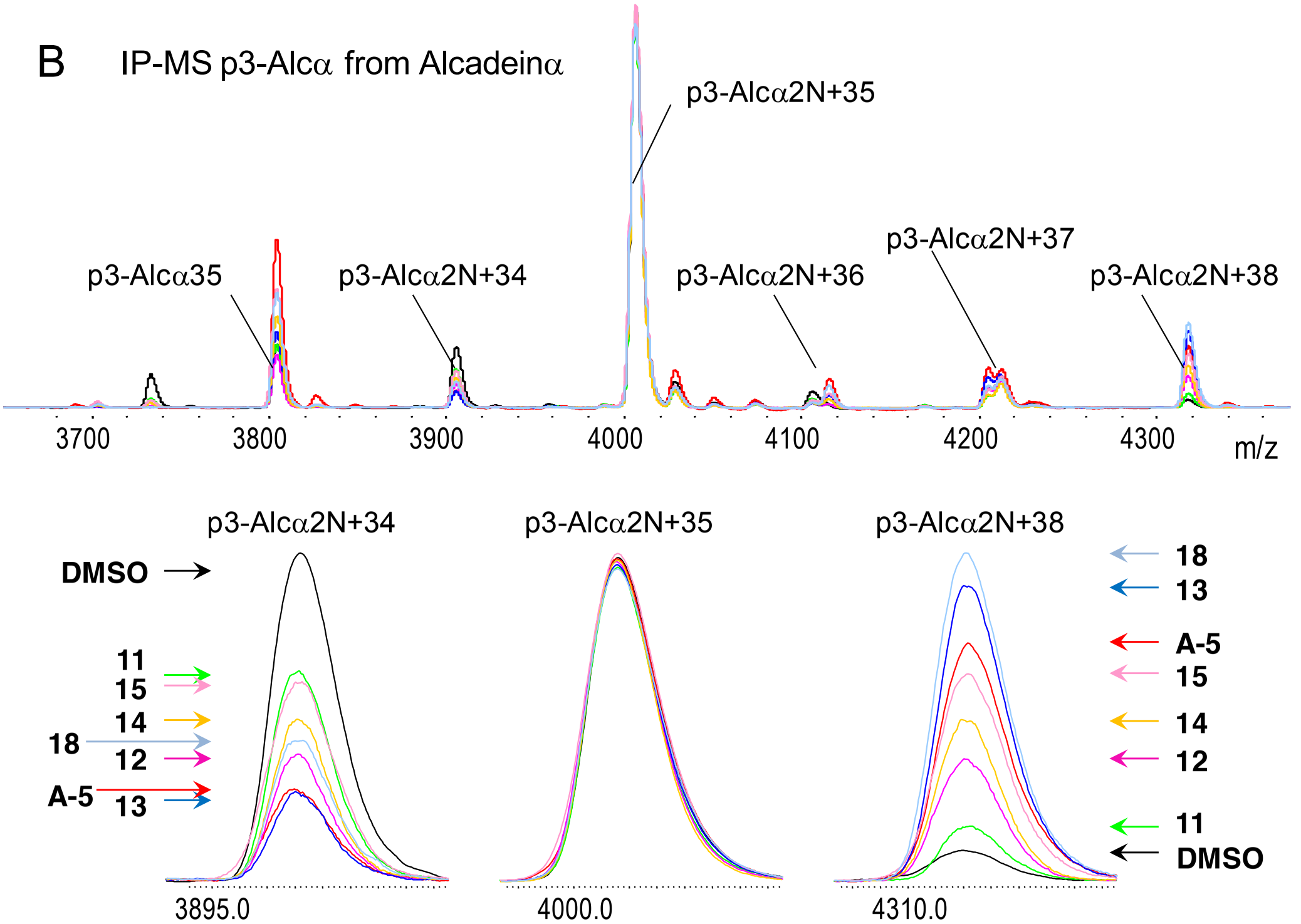

Portelius et al. Figure 6B

C

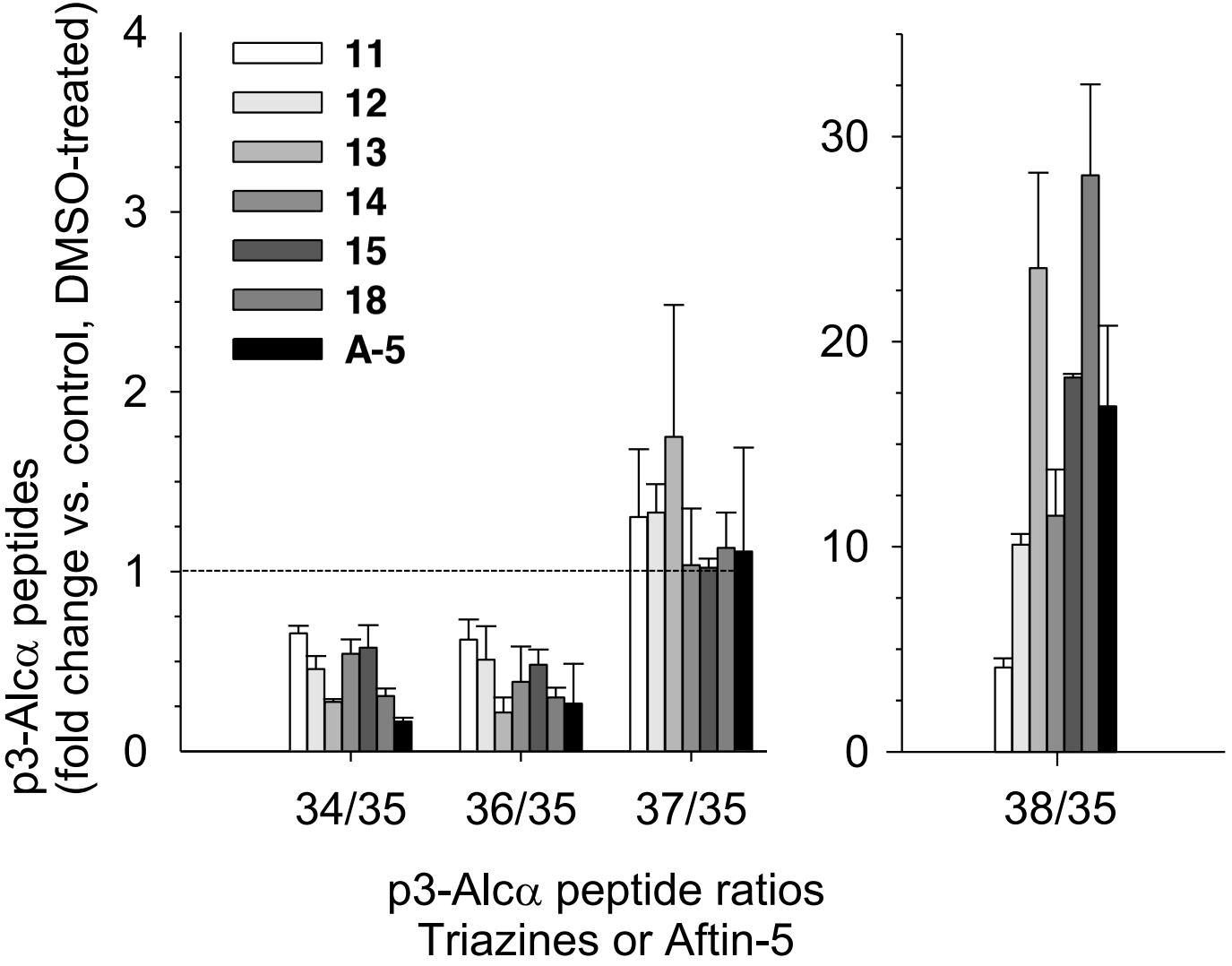

Portelius et al. Figure 6C

SUPPLEMENTARY INFORMATION

Specific triazine herbicides induce amyloid β 42 production

Erik **PORTELIUS**, Emilie **DURIEU**, Marion **BODIN**, Morgane **CAM**, Josef **PANNEE**, Charlotte **LEUXE**, Aloïse **MABONDZO**, Nassima **OUMATA**, Hervé **GALONS**, Jung Yeol **LEE**, Young-Tae **CHANG**, Kathrin **STÜBER**, Philipp **KOCH**, Gaëlle **FONTAINE**, Marie-Claude **POTIER**, Antigoni **MANOUSOPOULOU**, Spiros **GARBIS**, Adrian **COVACI**, Debby **VAN DAM**, Peter **DE DEYN**, Frank **KARG**, Marc **FLAJOLET**, Chiori **OMORI**, Saori **HATA**, Toshiharu **SUZUKI**, Kaj **BLENNOW**, Henrik **ZETTERBERG** and Laurent **MEIJER**

1. Supplementary Material & Methods

1.1. Triazines and other reagents

The main triazine herbicides (**1-36**) were obtained commercially from Fluka/ Sigma Aldrich (St. Quentin Fallavier, France). The flame retardant TTBP-TAZ (2,4,6-tris(2,4,6-tribromophenoxy)-1,3,5-triazine) (**37**) was from Sigma Aldrich (St. Quentin Fallavier, France).

Terbutryn and cybutryne metabolites and contaminants, 2-N-tert-butyl-6-(methylsulfanyl)-1,3,5-triazine-2,4-diamine (terbutryn impurity) (**39**), terbutylazine-2-hydroxy (**41**), 4-(tert-butylamino)-6-(ethylamino)-1,3,5-triazine-2-thiol (**42**), 4-(tert-butylamino)-6-(ethylamino)-1,3,5-triazine-2-thiol (**43**) and N,N'-dicyclopropyl-1,3,5-Triazine-2,4,6-triamine (cyromazine impurity) (**44**) were purchased from MicroCombiChem (Wiesbaden, Germany). Metabolite M13 (**40**) was synthesized by JL and YTC (not shown).

A panel of 236 triazines was selected in a large triazines library constructed as described previously [30, 31]. Twenty products displayed some activity (**45-65**) (Supplementary Table S5). Five triazines (**49, 66-69**) bearing a poly-ethylene glycol linker (2, 3 or 4 ethylene glycol moieties) were synthesized by JL and YTC (not shown).

Aftin-5 (**38**) (Adipogen International, San Diego, CA, USA) was synthesized as previously described [14]. Aftin-5 bearing a poly-ethylene glycol linker (5 ethylene glycol moieties) (**70**) was synthesized by NO and HG (not shown).

All compounds were solubilized as 100 mM stock solutions in 100% dimethylsulfoxide (DMSO) and diluted just prior use.

The γ-secretase modulator ('Torrey Pines' compound) was synthesized as previously described [14, 30, 31]. DMSO, Nonidet P-40, Tween-20, CHAPSO (3-[(3-cholamidopropyl)dimethylammonio]-2-hydroxy-1-propanesulfonate), dithiothreitol (DTT), bovine serum albumin (BSA), Na_2CO_3, $NaHCO_3$, citric acid monohydrate, $Na_2HPO_4.2H_2O$, H_2O_2, digitonin were purchased from Sigma Aldrich. Protease inhibitors mix (Complete) was obtained from Roche (Boulogne-Billancourt, France). Streptavidin-horseradish peroxidase (HRP) conjugate was purchased from Thermo Scientific Pierce (Brebières, France). o-Phenylenediamine dihydrochloride (OPD) tablets were from Invitrogen (St Aubin, France). γ-Secretase inhibitors BMS299897 and DAPT (*N*-[(3,5-difluorophenyl)acetyl]-L-alanyl-2-

phenyl]glycine-1,1-dimethylethyl ester) were obtained from Tocris Bioscience (Lille, France). β-secretase inhibitor IV was from Calbiochem (Molsheim, France).

1.2. Cell cultures: cell lines, primary neuron cultures, iPSCs-derived neurons & HEK293-alcadeinα cells

N2a-APP695 and CHO-7PA2 cell lines

N2a-APP695 cells (ECACC n° 89121404, lot 07/D/032) were cultured in Dulbecco's minimal essential medium (DMEM) / OptiMEM (1:1 v/v) (Invitrogen, Saint Aubin, France) containing 0.2 mg/mL Geniticin (Gibco, c/o Invitrogen) and 0.5% fetal bovine serum (FBS, Gibco) in a humidified, 5% CO_2 incubator. CHO-7PA2 cells (CHO cells stably expressing APP751 with the Val717Phe familial AD mutation, obtained from D.J. Selkoe, Harvard Medical School, Boston, USA) were cultured in DMEM/F12 (Invitrogen) + 0.5% FBS with Glutamax, Phenol Red and without HEPES. Cells were split routinely every 4/5 days. They were first rinsed with phosphate buffered saline (PBS) (Gibco) and detached from the plate bottom using 4 mL Versene (Gibco) at room temperature (RT) for 3-4 min. Eight mL of fresh medium were added to the cell suspension, and the mix was centrifuged for 3 min at 1,000 rpm. The cell pellet was resuspended in fresh medium before seeding (1/10 dilution) in new flasks.

Primary Rat Neuronal Cultures

Primary neuronal cultures were prepared from E18 OFA rats embryos brains (Charles River laboratories, L'Arbresle, France). All procedures were performed according to European law (EEC 86/609) and were approved by the local veterinary authorities (N° 12037). Primary cultures of cortical neurons were prepared according as described [65] with minor modifications. Dissociated neurons were plated onto poly-D-lysine (50 µg/mL) coated coverslips (14 mm diameter, Marienfeld GmbH, Lauda-Königshofen, Germany) into 12 wells culture plates (Costar, Corning NY, USA) at 10^5 cells/cm^2 for cortical neurons. All experiments were performed at 15 days *in vitro* (DIV). Briefly, cortices were dissected in Hank's Balanced Salt Solution (HBSS) containing 5 mM glucose (dissection medium). The medium was replaced 0.05% trypsin in 0.5 mM EDTA (Life Technologies, Grand island, NY, USA). Cortices were digested separately for 15 min at 37°C. After removing the trypsin, cortices were washed in dissection medium, and incubated in HBSS containing trypsin inhibitor (2 mg/mL, Sigma Aldrich, St Quentin Fallavier, France) and DNAse I (0.05%, Sigma) for 3 minutes at 37°C. Cortices were washed in dissection medium, taken up in few mL of dissection medium and gently triturated by passing through a 1 mL ART® filter tip. Cells were counted and seeded at a density of 10^5 cells/cm^2 into 12 wells culture plates (Costar) in plating medium (DMEM medium containing 10% heat-inactivated horse serum (Life Technologies)). Wells contained acid-washed glass coverslips (14 mm diameter, Marienfeld) which had been precoated with 50 µg/mL poly-D-lysine (Sigma). Cultures were left to attach at 37°C with 5% CO_2. After 2 h, the plating medium was replaced with Neurobasal containing 2 mM glutamine, 1 mM sodium pyruvate, 10 µg/mL penicillin and streptomycin, and 2% B27 supplement (Life Technologies) (culture medium). After 4 days, cytosine arabinoside (Sigma, 3 µM final concentration) was added to suppress glial cell proliferation. Cultures were fed twice a week by adding a quarter of the volume of fresh culture medium (after removal of the same volume). At DIV 15th, neurons were incubated in culture medium (MEM 1X (Life Technologies), HEPES buffer 1M 1,5%

(Life Technologies) and NaOH (Sigma) up to pH 7,3) containing 100 µM herbicides or 100 µM aftin-5 (ManRos Therapeutics, Roscoff, France) or vehicle (0,1% sterile DMSO, Sigma) for 18 hours. At the end of the treatment, secreted $A\beta_{38}$, $A\beta_{40}$ and $A\beta_{42}$ peptides in conditioned medium were quantified by a sandwich immunoassay using the Meso Scale Discovery SECTOR Imager 2400. All reagents were from Meso Scale Discovery (Rockeville MD, USA).

Human iPSCs-derived neuronal cultures

Induced pluripotent stem cells (iPSCs) from 33-year old healthy male (AβPP WT, wild-type) and 55-year old female harboring a lysine 724 to asparagine mutation in AβPP (AβPP K724N mutation) have been generated and characterized previously [37, 38]. From iPSCs we generated long-term self-renewing neuroepithelial stem cells (lt-NES cells), a homogeneous population which can be continuously propagated in the presence of FGF2 and EGF. To that end, 4-day-old embryoid bodies were transferred to polyornithine-coated tissue culture dishes and propagated in N2 medium (DMEM/F12 high glucose; N2 supplement, both Life Technologies, Darmstadt, Germany). Within 10 days, neural island consisting of neural rosettes and neural tube-like structures developed in the embryoid body outgrowth. These islands were mechanically isolated by separation from the surrounding cells with a scalpel. Isolated clusters where further propagated for 2 days as free-floating neurospheres in N2 medium containing 10 ng/mL FGF2 and 10 ng/mL EGF (both R&D Systems, Wiesbaden, Germany) and 1 µL/mL B27 Supplement (Life Technologies; short: N2 FEB medium). Spheres were triturated into single cells by incubating the spheres with trypsin/EDTA for 10 min followed by gentle dissociation with a 1.000 µL pipette tip. Cells were plated on polyornithine (Sigma Aldrich) and laminin (Life Technologies) precoated plastic dishes. Passaging of the cells was performed when cells had reached full confluence (normally every 3-4 days) at a 1:2 – 1:3 ratio using trypsin/EDTA. Medium was changed every other day while growth factors were added on a daily basis.

Neuronal differentiation was performed by plating 300,000 and 1,000,000 cells per well of a Geltrex (Life Technologies; diluted 1:50)-precoated 12-well plate or 6-well plate, respectively, in N2 FEB medium. The following day, the medium was changed to terminal differentiation medium containing DMEM/F12 and MACS Neuro Medium (Miltenyibiotec, Bergisch Gladbach, Germany) mixed at a 1:1 ratio and supplemented with 1:200 N2 supplement, 1:100 B27 supplement and 300 ng/mL cAMP (Sigma Aldrich). Medium was changed every other day.

Compound treatment was performed on neuronal cultures differentiated for at least 4 weeks. Cells were pretreated for 16 h with compound containing medium (all compounds at 100 µM in 500 µL medium/ 12-well plate and 1,5 ml medium/ 6-well plate). Solvent only (DMSO) was used as control. Medium was replaced (same volume with freshly added compounds) and supernatants and lysates were harvested 24 h later. Supernatants were directly frozen in liquid nitrogen until analyzed. $A\beta_{42}$ and $A\beta_{40}$ in the supernatants were analyzed by ELISA (Meso Scale Discovery, Rockeville MD, USA) and normalized to the protein content of the cell pellet.

HEK293-alcadeinα cell culture and Alcadein fragments analysis

The full-length human Alcadeinα1 (Alcα) open reading frame [24] was subcloned into the HindIII and XbaI sites of pcDNA3.1 (Hygro+) vector (Invitrogen/Thermo Fisher Scientific,

Carlsbad, CA), transfected into HEK293 cells with Lipofectamine 2000 (Invitrogen/Thermo Fisher Scientific, Carlsbad, CA), and cells stably expressing Alcα were cloned. The cells cultured in dish coated with poly-L-lysine were treated with Aftin-5 or triazines (100 μM) for 24 h. The secreted p3-Alcα were recovered from the cultured medium by immunoprecipitation with anti-p3-Alcα UT175 antibody, an antibody raised to an antigen peptide composed of Cys plus the human Alcα1 839-851 sequence, using Protein G-Sepharose beads (GE Healthcare, Little Chalfont, UK). The beads were sequentially washed and samples were eluted with trifluoroacetic acid/acetonitrile/water (1:20:20) saturated with sinapinic acid, and subject to MALDI-TOF-MS analysis using an Ultraflex II TOF/TOF (Bruker Daltonics, Bremen, Germany). Molecular masses were calibrated using the peptide calibration standard (Bruker Daltonics) [25].

1.3. Transient transfections with AβPP truncation mutants

We used the human APP cDNA for all the experiments presented and the truncation mutants were generated by PCR using standard molecular techniques.

Briefly, full-length human APP cDNA was previously subcloned by using standard PCR and TA cloning molecular techniques, into the pcDNA3.1(+) plasmid (Invitrogen, Carlsbad, CA) at BglII/BstXI restriction sites. Truncated APP mutants were subcloned from TA by EcoR1/EcoR1 restriction sites into APP containing pcDNA3.1 (+) plasmid.

Forward oligonucleotide for:

T1-T6: 5'-TAT ATA AGA TCT CTG AAG TGA AGA TGG ATG C-3'

Reverse oligonucleotides for:

T1: 5'-TAT ATA CCA GAC TAC TGG CTA GGT GAC AGC GGC GTC AAC-3'
T2: 5'-TAT ATA CCA GAC TAC TGG CTA CAC ACC ATG ATG AAT GGA-3'
T3: 5'-TAT ATA CCA GAC TAC TGG CTA CTG TTT CTT CTT CAG CAT -3'
T4: 5'-TAT ATA CCA GAC TAC TGG CTA CAG CAT CAC CAA GGT GAT-3'
T5: 5'-TAT ATA CCA GAC TAC TGG CTA CAC CAA GGT GAT GAC GAT -3'
T6: 5'-TAT ATA CCA GAC TAC TGG CTA CAA GGT GAT GAC GAT CAC -3'

N2a cells were maintained in growing medium (50% DMEM, 50% OPTI-MEM) supplemented with 5% fetal bovine serum (vol/vol). Transfections were carried using Fugene6 according to the manufacturer instructions. For experiments, cells were plated in 6-well plates at a density of 4×10^5 cells per well. Cells were grown to about 40% confluence and then transfected with relevant plasmid constructs using FuGENE6 (Roche, Indianapolis). 48 h after transfection, cells were treated for 24 h with various triazines. Supernatants were collected for Aβ42 measurements and cells were harvested for protein quantification.

1.4. Amyloids assays

Amyloids were measured by different methods according to the different cell types:

- Primary rat neuronal cultures and human iPSCs-derived neuronal cultures: Meso Scale Discovery sandwich ELISA immunoassay.
- N2a cells transfected with various APP C-terminal truncated mutants: BioSource International ELISA assay (see below).

- N2a-APP695 and CHO-7PA2 cell lines: an in-house sandwich ELISA assay described below, as well as tandem mass spectrometry (MS/MS) (see below) and immunoprecipitation / mass spectrometry (IP-MS) (see below).

In-house ELISA capture assay [14]

N2a-APP695 or CHO-7PA2 cells were seeded at 10,000 cells/well in a 96 well plate with modified media (0.5% FBS) and incubated overnight. Cells were treated with fresh media and different compounds (equal quantity of DMSO), then incubated for 18 h in a humidified, 5% CO_2 incubator. The plate was finally centrifuged to remove cell fragments before collecting supernatant samples for amyloids levels determination (see below). To determine the amount of secreted Aβ peptides in the primary rat neuron culture medium, 15 days culture medium was discarded and replaced by fresh media which was collected after 18 h incubation.

$Aβ_{38}$, $Aβ_{40}$, $Aβ_{42}$ levels were measured in a double antibody sandwich ELISA using a combination of monoclonal antibody (mAb) 6E10 (Covance c/o Ozyme, Montigny-le-Bretonneux, France) and biotinylated polyclonal $Aβ_{38}$ [66], $Aβ_{40}$ or $Aβ_{42}$ [67] antibodies (provided by Dr. P.D. Mehta, Staten Island, USA). Briefly, 100 µL mAb 6E10 diluted in carbonate-bicarbonate buffer (buffer (0.015 M Na_2CO_3 + 0.035 M $NaHCO_3$) pH 9.6), was coated in the wells of microtiter plates (Maxisorp, Nunc,ThermoFisher Scientific, Illkirch, France) and incubated overnight at 4°C. The plates were washed with PBST (PBS containing 0.05% Tween-20) and blocked for 1 h with 1% BSA in PBST to avoid non-specific binding. Each of the $Aβ_{38}$, $Aβ_{40}$ or $Aβ_{42}$ antibodies did not cross-react with the other amyloid peptides (data not shown). Standard curves were prepared with synthetic amyloids and each of the three antibodies. Fitting was performed using a 4 parameters sigmoid equation (SigmaPlot, Systat, Macon, France).

Typically, the first day, the cells were detached of the flask with Versene, centrifuged during 3 minutes at 1000 rpm and suspended in 10 mL of medium. The cells were counted and seeded in 6 well plates at 200,000 cells/well. The medium used were DMEM/F12 supplemented with 0.5% FBS for the CHO-7PA2 cells and DMEM/Optimem (1:1) supplemented with 0.5% FBS for N2aAPP695 cells. The second day, the cells were treated for 24 h with 100 µM Aftin 5 or Triazine in a final concentration of DMSO of 0.1%. Control cells were also exposed to 0.1% DMSO. The volume final of medium was 2 mL. The third day, after the 24 h treatment, the plates were agitated slowly and 2 mL of medium were collected in one tube (3 tubes per condition). The tubes were inverted and 200 µL were removed for ELISA analysis. The remaining 1.8 mL were frozen at -80°C.

Following a washing step, experimental samples were added into the wells and incubation was carried out for 2 h at RT and overnight at 4°C. Plates were washed before incubation with biotinylated polyclonal antibody diluted in PBST + 0.5% BSA at RT for 75 min. After a washing step, streptavidin-HRP conjugate, diluted in PBS + 1% BSA, was added and incubation was carried out for 45 min at RT. After washing, 100 µl OPD in citrate buffer (0.049 M citric acid monohydrate + 0.1 M $Na_2HPO_4.2H_2O$ + 1 mL H_2O_2 30%/L) pH 5.0 were added. The reaction was stopped after 15 min with 100 µL 1 N sulfuric acid. The optical density was measured at 490 nm in a microELISA reader (BioTek Instrument, El 800, Gen 5 software).

BioSource International ELISA assays and data analysis

β Amyloid 1-40 or 1-42 Colorimetric Elisa kits were used for cells transfected with human full length APP and its truncation mutants. After immobilization of total Aβ from media, Aβ40/42 peptide determinations were made by sandwich ELISA (BioSource International, Camarillo, CA). Aβ levels were normalized to total protein levels after cell recovery. Cells were recovered with 100 µL of RIPA buffer (0.15 mM NaCl/0.05 mM Tris·HCl, pH 7.2/1% Triton X-100/1% sodium deoxycholate/0.1% SDS), incubated for 30 min on ice, and centrifuged at 10,000 × g for 20 min at 4°C. $A\beta_{40}$ and $A\beta_{42}$ standard curves were plotted as a sigmoidal dose-response curve (variable slope) by using GraphPad Prism ver. 4.0. Data presented are the results of at least three independent experiments done in triplicate.

Absolute quantification of amyloids by tandem mass spectrometry (MS/MS)

Solid phase extraction, liquid chromatography (LC) and MS/MS analysis of Aβ species was performed as described previously [34, 35] with the following modifications. Standard curves for $A\beta_{38}$ and $A\beta_{42}$ were prepared at 0.15, 0.5, 1, 2, 3 and 4 ng/mL while $A\beta_{40}$ was prepared at 15, 50, 100, 200, 300 and 400 ng/mL using unlabeled peptides (rPeptide) in DMEM/F12 supplemented with 0.5% FBS. Uniformly labeled ^{15}N-$A\beta_{38}$, $A\beta_{40}$ and $A\beta_{42}$ peptides (rPeptide) were added to a final concentration of 1.6 ng/mL in calibrators and unknown samples as internal standards. Standard curves were constructed using the unlabeled to ^{15}N-Aβ peak area ratios and fitted using linear regression. All standard curves were linear and had an R^2 value greater than 0.998. Concentrations of unknowns were extrapolated from the standard curves using the peak area ratio of endogenous to ^{15}N-Aβ.

Amyloids profile analysis by immunoprecipitation / mass spectrometry (IP-MS)

Immunoaffinity capture of Aβ species was combined with matrix-assisted laser desorption/ionization time-of-flight (MALDI-TOF) MS for analyzing a variety of Aβ peptides in a single analysis as described [68]. In brief, the anti-Aβ antibodies 6E10 and 4G8 were separately coupled to magnetic beads. After washing of the beads, the 4G8 and 6E10-coated beads were used in combination for immunoprecipitation. After elution of the immune-purified Aβ peptides, analyte detection was performed on an UltraFlextreme MALDI TOF/TOF instrument (Bruker Daltonics). For each peak the areas were normalized against the sum for all the Aβ peaks in the spectrum followed by averaging of results for separately determined duplicate samples [36].

1.5. Cell viability

To measure cell viability, the MTS (3-(4,5-dimethylthiazol-2-yl)-5-(3-carboxymethoxyphenyl)-2-(4-sulfophenyl)-2*H*-tetrazolium) assay (CellTiter 96 AQueous One Solution Cell Proliferation Assay, Promega, Charbonnières-les-Bains, France) was used in the same wells as the capture ELISA assay. Briefly, 20 µL of MTS reagent was added in each well containing 100 µL of media and incubation then proceeded for 3 h (37°C, 5% CO_2 and 95% humidity). Measurements were made at OD 490Δ630 nm using a microELISA reader.

2. Supplementary Tables

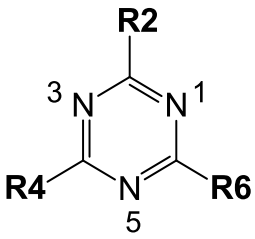

#	Triazines	2	4	6
1	Atrazine	-Cl	-NH-C_2H_5	-NH-$CH(CH_3)_2$
2	Simazine	-Cl	-NH-C_2H_5	-NH-C_2H_5
3	Propazine	-Cl	-NH-$CH(CH_3)_2$	-NH-$CH(CH_3)_2$
4	Cyanazine	-Cl	-NH-C_2H_5	-NH-$C(CH_3)_2CN$
5	Terbuthylazine	-Cl	-NH-C_2H_5	-NH-$C(CH_3)_3$
6	Sebuthylazine	-Cl	-NH-C_2H_5	-NH-$CH(CH_3)$-C_2H_5
7	Atraton	-OCH_3	-NH-C_2H_5	-NH-$CH(CH_3)_2$
8	Terbumeton	-OCH_3	-NH-C_2H_5	-NH-$C(CH_3)_3$
9	Prometon	-OCH_3	-NH-$CH(CH_3)_2$	-NH-$CH(CH_3)_2$
10	Simetryn	-SCH_3	-NH-C_2H_5	-NH-C_2H_5
11	Ametryn	-SCH_3	-NH-C_2H_5	-NH-$CH(CH_3)_2$
12	Prometryn	-SCH_3	-NH-$CH(CH_3)_2$	-NH-$CH(CH_3)_2$
13	Dipropetryn	-SC_2H_5	-NH-$CH(CH_3)_2$	-NH-$CH(CH_3)_2$
14	Terbutryn	-SCH_3	-NH-C_2H_5	-NH-$C(CH_3)_3$
15	Cybutryne	-SCH_3	-NH-cycloC_3H_5	-NH-$C(CH_3)_3$
16	Aziprotryn	-SCH_3	-N=N^+=N^-	-NH-$CH(CH_3)_2$
17	Desmetryn	-SCH_3	-NH-CH_3	-NH-$CH(CH_3)_2$
18	Dimethametryn	-SCH_3	-NH-C_2H_5	-NH-$CH(CH_3)$-$CH(CH_3)_2$
19	Methoprotryn	-SCH_3	-NH-$CH(CH_3)_2$	-NH- $(CH_2)_3$-OCH_3
20	Hydroxyatrazine	=O	-NH-C_2H_5	-NH-$CH(CH_3)_2$
21	Desethylhydroxy-atrazine	-OH	-NH_2	-NH-$CH(CH_3)_2$
22	Ammmeline	-OH	-NH_2	-NH_2
23	Didealkylatrazine	-Cl	-NH_2	-NH_2
24	Desethylatrazine	-Cl	-NH_2	-NH-$CH(CH_3)_2$
25	Deisopropylatrazine	-Cl	-NH-C_2H_5	-NH_2
26	Hexazinone *	=O	=O	- $N(CH_3)_2$
27	Terbumeton-desethyl	-OCH_3	-NH_2	-NH-$CH(CH_3)$-C_2H_5
28	Thifensulfuron-methyl	-OCH_3	-CH_3	-NH-CO-NH-SO_2-X1
29	Iodosulfuron-methyl-sodium	-OCH_3	-CH_3	-NH-CO-NH-SO_2-X2
30	Chlorosulfuron	-OCH_3	-CH_3	-NH-CO-NH-SO_2-X3
31	Tribenuron-methyl	-OCH_3	-CH_3	-$N(CH_3)$-CO-NH-SO_2-X4
32	Triasulfuron	-OCH_3	-CH_3	-NH-CO-NH-SO_2-X5
33	Triflusulfuron-methyl	-OCH_2-CF_3	-$N(CH_3)_2$	-NH-CO-NH-SO_2-X6
34	Cinosulfuron	-OCH_3	-OCH_3	-NH-CO-NH-SO_2-X7
35	Metsulfuron-methyl	-OCH_3	-CH_3	-NH-CO-NH-SO_2-X8
36	Trietazine	-Cl	-$N(C_2H_5)_2$	-NH-$CH(CH_3)_2$
37	TTBP-TAZ	2,4,6-tribromophenoxy	2,4,6-tribromophenoxy	2,4,6-tribromophenoxy

* N1 = - phenyl ; N3= - CH_3

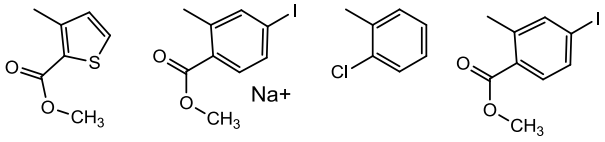

X1 **X2** **X3** **X4**

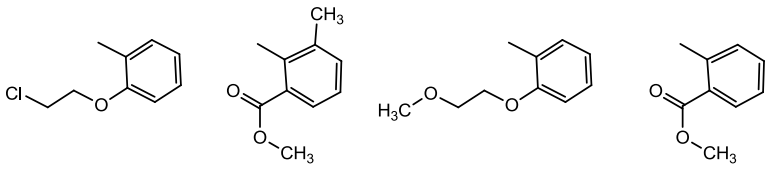

X5 **X6** **X7** **X8**

Table S1. Structure of the triazines tested.

#	Triazines	N2a-APP695 ($A\beta_{42}$ fold change)	CHO-7PA2 ($A\beta_{42}$ fold change)
1	Atrazine	2.39 ± 0.17	1.64 ± 0.08
2	Simazine	1.42 ± 0.13	1.04 ± 0.12
3	Propazine	2.18 ± 0.42	1.15 ± 0.07
4	Cyanazine	1.39 ± 0.11	0.93 ± 0.07
5	Terbuthylazine	2.91 ± 0.26	1.92 ± 0.19
6	Sebuthylazine	2.65 ± 0.17	1.89 ± 0.14
7	Atraton	1.29 ± 0.10	1.21 ± 0.15
8	Terbumeton	2.66 ± 0.20	2.57 ± 0.12
9	Prometon	2.05 ± 0.32	2.00 ± 0.17
10	Simetryn	2.09 ± 0.23	1.86 ± 0.18
11	**Ametryn**	**3.39 ± 0.31**	**3.39 ± 0.25**
12	**Prometryn**	**5.63 ± 0.63**	**5.65 ± 0.17**
13	**Dipropetryn**	**10.03 ± 0.97**	**5.51 ± 0.62**
14	**Terbutryn**	**7.23 ± 0.56**	**6.29 ± 0.95**
15	**Cybutryne**	**6.81 ± 0.81**	**5.71 ± 0.37**
16	Aziprotryn	2.16 ± 0.29	1.73 ± 0.04
17	Desmetryn	1.60 ± 0.13	1.76 ± 0.23
18	**Dimethametryn**	**6.67 ± 0.62**	**5.52 ± 0.48**
19	Methoprotryn	2.72 ± 0.21	2.88 ± 0.11
20	Hydroxyatrazine	1.02 ± 0.14	1.02 ± 0.07
21	Desethylhydroxy-atrazine	1.04 ± 0.19	1.09 ± 0.10
22	Ammeline	0.96 ± 0.24	0.93 ± 0.10
23	Didealkylatrazine	0.86 ± 0.15	0.79 ± 0.06
24	Desethylatrazine	1.34 ± 0.19	1.22 ± 0.11
25	Desisopropylatrazine	1.31 ± 0.26	1.15 ± 0.09
26	Hexazinone	0.90 ± 0.19	1.08 ± 0.15
27	Terbumeton-desethyl	1.28 ± 0.22	1.26 ± 0.14
28	Thifensulfuron-methyl	0.85 ± 0.09	0.97 ± 0.14
29	Iodosulfuron-methyl-sodium	0.99 ± 0.12	1.05 ± 0.04
30	Chlorosulfuron	0.91 ± 0.08	1.05 ± 0.17
31	Tribenuron-methyl	1.21 ± 0.14	1.11 ± 0.06
32	Triasulfuron	0.85 ± 0.21	0.92 ± 0.13
33	Triflusulfuron-methyl	0.82 ± 0.12	0.78 ± 0.08
34	Cinosulfuron	0.77 ± 0.11	0.82 ± 0.16
35	Metsulfuron-methyl	0.69 ± 0.11	0.86 ± 0.11
36	Trietazine	0.46 ± 0.34	0.85 ± 0.21
37	TTBP-TAZ	1.13 ± 0.09	1.01 ± 0.14
38	**Aftin-5**	**6.24 ± 0.67**	**4.34 ± 0.61**

Table S2. Effect of 37 triazines on extracellular amyloid $A\beta_{42}$ production by N2a-APP695 and CHO-7PA2 cells. Cells were treated with 100 μM of each compound for 18 h and cell supernatants were collected for extracellular $A\beta_{42}$ levels measurement by an ELISA assay. Aftin-5 was used as positive control and corresponding volume of vehicle (DMSO) was used as a negative control. Levels are expressed as fold change ± standard error of $A\beta_{42}$ level over the $A\beta_{42}$ level of control, vehicle-treated cells. Average of two experiments performed in triplicate (representative of four independent experiments). In bold, products inducing >3 fold increase of $A\beta_{42}$ production. TTBP-TAZ, 2,4,6-tris(2,4,6-tribromophenoxy)-1,3,5-triazine. Products were tested at 1, 10 and 100 μM, but only results with 100 μM are shown here to also show the inactive products. A dose-dependent effect was often seen with the active compounds.

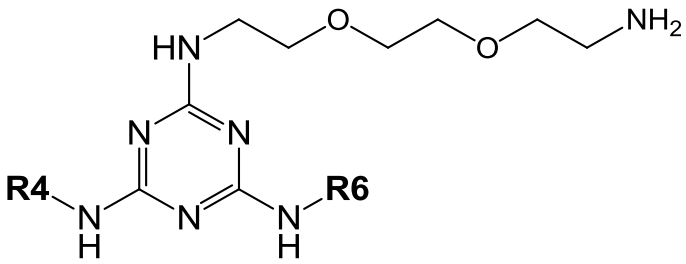

#	Triazines	R_2	R_4	R_6	N2a-APP695 ($A\beta_{42}$ fold change)
45	AA9-E02 *	-NH-$(CH_2)_2$-$(OCH_2CH_2)_2$-NH_2	-$(CH_2)_2$-Ph	-NH-*i*-Pr	1.29 ± 0.01
46	**AA9-E03**	〃	-$(CH_2)_2$-Ph	-NH-C_4H_9	**3.14 ± 0.15**
47	AA9-E04	〃	-$(CH_2)_2$-Ph	-N-$(C_4H_9)_2$	1.59 ± 0.06
48	AA9-E05	〃	-$(CH_2)_2$-Ph	-NH-cyclohexyl	2.31 ± 0.15
49	**AA9-F03**	〃	-CH_2-Bn-p-OCH_3	-NH-C_4H_9	**5.63 ± 0.16**
50	**AA9-F08**	〃	-CH_2-Bn-p-OCH_3	-piperidine	**3.37 ± 0.17**
51	**AA9-G03**	〃	- Ph-p-OCH_3	-NH-C_4H_9	**4.29 ± 0.32**
52	AA9-G04	〃	-Ph-p-OCH_3	-N-$(C_4H_9)_2$	2.20 ± 0.13
53	AA9-G05	〃	-Ph-p-OCH_3	-NH-cyclohexyl	2.74 ± 0.05
54	AA9-G06 *	〃	-Ph-p-OCH_3	-NH-CH_2-CH=CH_2	2.34 ± 0.38
55	**AA9-G07**	〃	-Ph-p-OCH_3	-NH-CH_2-(2-tetrahydrofuran)	**3.07 ± 0.39**
56	AA9-G08	〃	-Ph-p-OCH_3	-piperidine	2.63 ± 0.43
57	AA9-H03	〃	-CH_2-$CH(OH)_2$	-NH-C_4H_9	2.68 ± 0.40
58	AA10-B02	〃	-CH_2-Bn-p-OCH_3	-NH-C_8H_{17}	2.88 ± 0.12
59	**AA10-B10**	〃	-CH_2-Bn-p-OCH_3	-NH-p-F-Bn	**4.43 ± 0.11**
60	AA10-C10	〃	-Ph-p-OCH_3	-NH-p-F-Bn	2.28 ± 0.36
61	**AA11-A09**	〃	-CH_2-Bn	-NH-CH(isopropyl)-CO-OCH_3	**3.29 ± 0.58**
62	AA11-B08	〃	-CH_2-Bn-p-OCH_3	-NH-CH(benzyl)-CO-OCH_3	2.71 ± 0.47
63	**AA11-B09**	〃	-CH_2-Bn-p-OCH_3	-NH-CH(*i*-Pr)-CO-OCH_3	**3.03 ± 0.17**
64	AA11-E08	〃	-CH_2-Bn	-p-tBut-Ph	2.27 ± 0.15
65	AA11-F08	〃	-CH_2-Bn-p-OCH_3	-p-tBut-Ph	2.14 + 0.10
66	A1	-S-$(CH_2)_2$-$(OCH_2CH_2)_3$-NH_2	-NH-*i*-Pr	-NH-*i*-Pr	**8.17 ± 0.37**
67	B1	-S-$(CH_2)_2$-$(OCH_2CH_2)_4$-NH_2	-NH-*i*-Pr	-NH-*i*-Pr	**4.17 ± 0.89**
68	D1	-NH-$(CH_2)_2$-$(OCH_2CH_2)_2$-NH_2	-NH-*i*-Pr	-NH-*i*-Pr	2.22 ± 0.15
69	C1	-NH-$(CH_2)_2$-$(OCH_2CH_2)_3$-NH_2	-NH-*i*-Pr	-NH-*i*-Pr	2.63 ± 1.08
70	Aftin-5L				**5.10 ± 0.57**

Table S3. Effect of 21 products selected from a triazine library on extracellular Amyloid $A\beta_{42}$ production by N2a-APP695. N2a-APP695 **c**ells were first treated with 10 and 100 µM of 236 triazines for 18 h and cell supernatant was collected for extracellular $A\beta_{42}$ levels measurement by an ELISA assay. The library was screened in triplicate, and active products (> 3 fold increase in Aβ42 production) were tested at 100 µM on N2a-APP695 **c**ells in three independent experiments. Levels are expressed as fold change of $A\beta_{42}$ level over the $A\beta_{42}$ level of control, vehicle-treated cells. Average ± errors bars represent standard error of triplicate values. *, 33 µM. Aftin-5 was used as positive control, and corresponding volume of vehicle (DMSO) was used as a negative control.

3. Supplementary figures

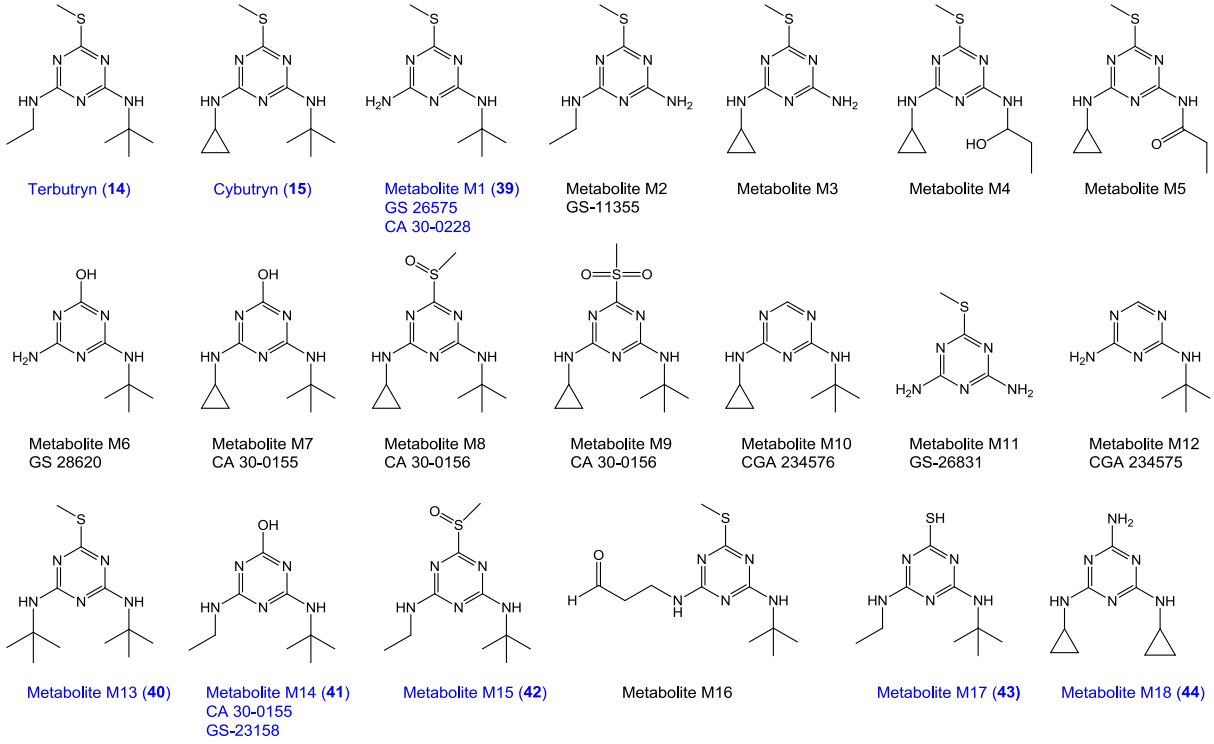

Figure S1. Structure of main terbutryn and cybutryn metabolites. Blue, products which were available for evaluation in the cellular $A\beta_{42}$ production assay.

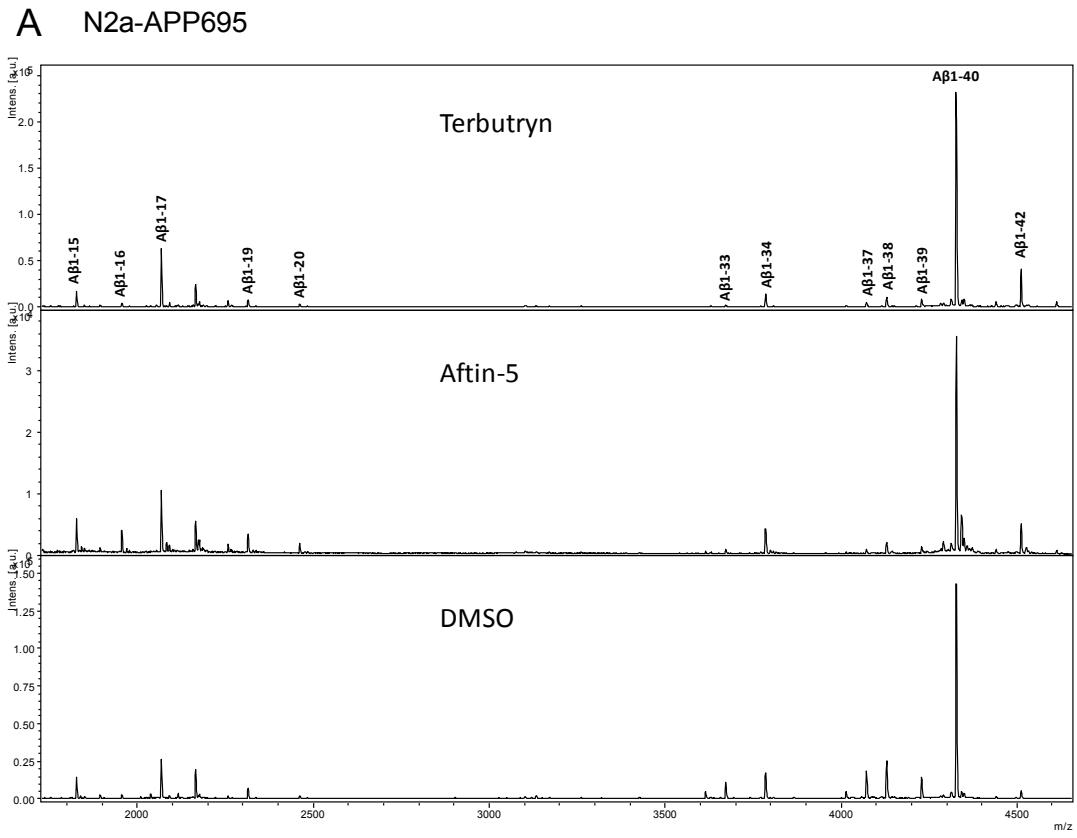

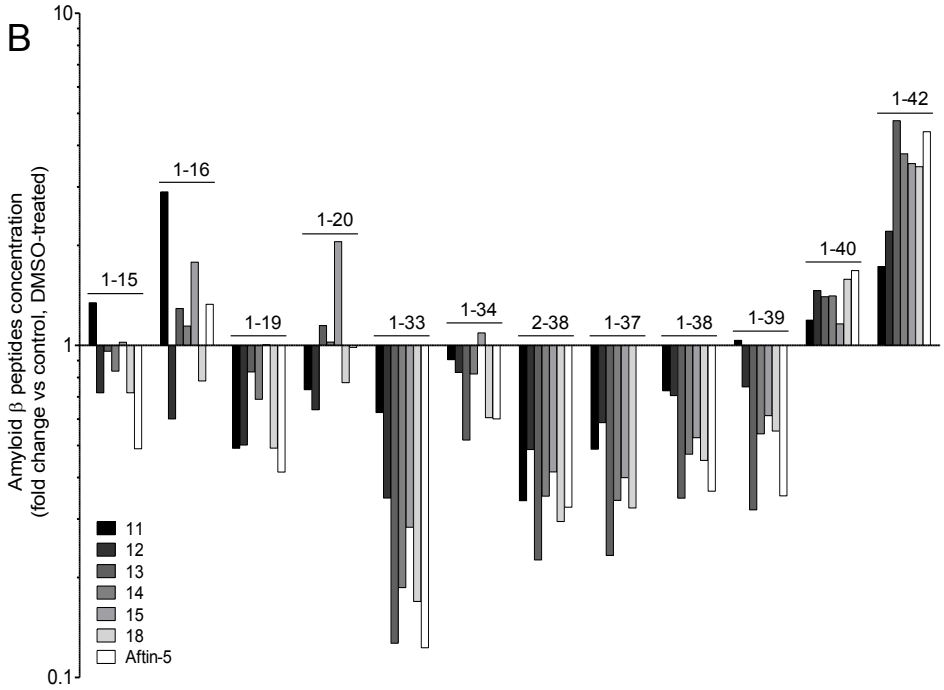

Figure S2. Pattern of amyloid peptides produced by N2a-APP695 cells exposed to triazines. Cells were treated for 18 h with DMSO, 100 µM of each triazine or aftin-5. Cell supernatants were collected and analyzed as described. **A**. Example spectra of supernatants amyloid profiles from N2a-APP695 cells exposed to DMSO, aftin-5 or terbutryn. **B.** Quantification of all amyloid peptides in N2a-APP695 cell supernatants (Log of fold change in triazine or aftin-5 treated cells over control, DMSO-treated cells).

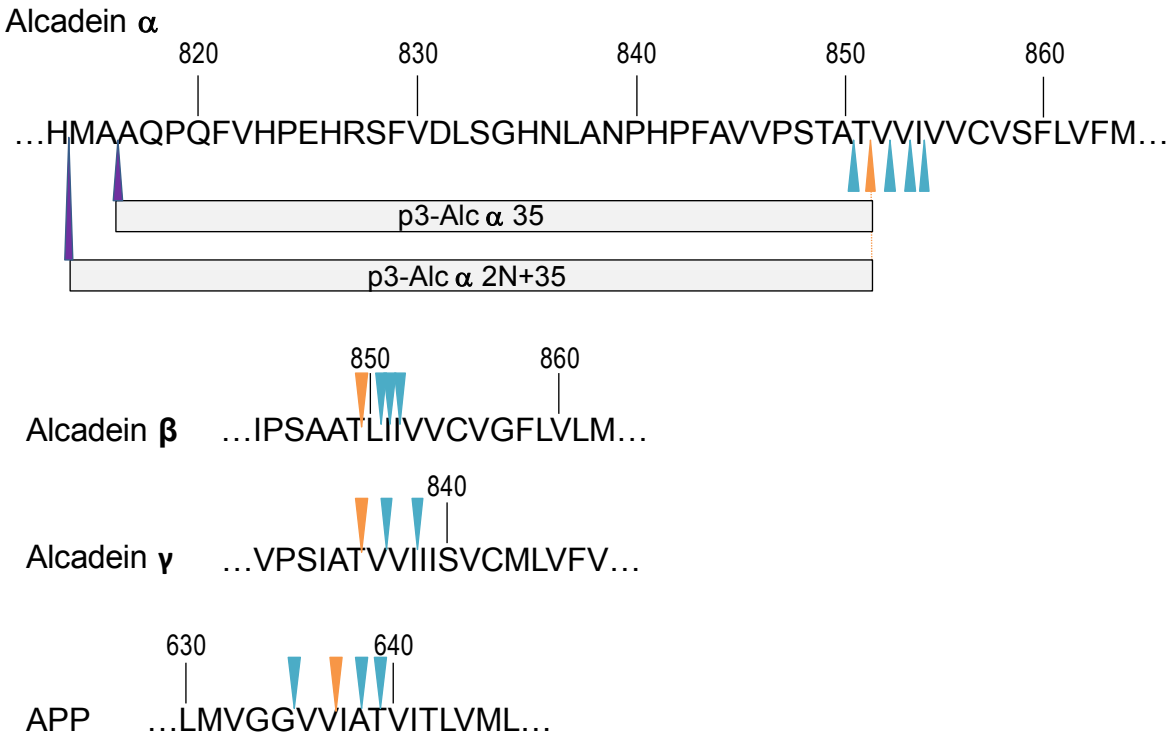

Figure S3. γ-Secretase cleavage sites in Alcadeins and AβPP.